UNIVERSITY OF CALIFORNOA,

IRVINE

Synthesis and Characteristics of Gold Nanorod

THESIS

submitted in partial satisfaction of the requirements

for the degree of

MASTER OF MATERIAL SCIENCE

in Materials Science and Engineering

by

Jiayu Cao

Thesis Committee:

Professor Regina Ragan, Chair

Professor James Earthman

Professor Daniel Mumm

2016

TABLE OF CONTENT

LIST OF FIGURES

Page

LIST OF TABLES

ACKNOWLEDGEMENTS

I would like to express the deepest appreciation to my committee chair, Professor Regina Ragan, who has the attitude and the substance of a genius: she continually and convincingly conveyed a spirit of adventure in regard to research and scholarship, and an excitement in regard to teaching. Without her guidance and persistent help this dissertation would not have been possible.

I would like to thank my committee members, Professor James Earthman and Professor Daniel Mumm, whose work demonstrated to me that concern for global affairs supported by an “engagement” in comparative literature and modern technology should always transcend academia and provide a quest for our times.

ABSTRACT OF THE THESIS

Synthesis and Characteristics of Gold Nanorod

By

Jiayu Cao

Master of Engineering in Material Science and Engineering

University of California, Irvine, 2016

Professor Regina Ragan, Chair

During recent decades gold nanorod has been found very interesting due to their optical and thermal characteristics which make them suitable for different applications. Many interesting applications are optical application because of rod's strong, special range of plasmon resonances, such as biotechnological imaging and sensing, surface-enhanced raman scattering and metamaterials, and these applications' performances can be impaired by polydispersity and low yield of gold nanorod when using seed-mediated method. Since seed-mediate approach is the most convenient and cheap method making gold nanorod, so it is necessary to find ways to optimize this method. In this research, first, we focus on relationship between shapes of gold nanorods and several factors exist in forming process due to its unique surface plasmon resonance and try to find an effect way to optimize this formation. Second, we put an effort to explain the mechanism of whole formation of rods by designing experiments testing rods' properties and directly observing rods through SEM. Experimental results are shown as we predicted, strong acid environment with slowly stirring during rods forming process can optimize seed-mediate approach and mechanism of it is: growth isotropically at first, when seeds' size are up to 6nm, they change to growth anisotropically due to CTA−Br−Ag^{+} capping agents forcing rods growth in specific direction.

CHAPTER 1
INTRODUCTION

This chapter is focus on introducing basic knowledge of nanomaterials and physical properties such as surface plasmon resonance which are necessary for this thesis. This chapter is divided into two parts: first, make an introduction of nanomaterials and focus on gold nanomaterials. Correlations between shape, size, will be made with optical properties of nanomaterial. Second, show the project objectives and organization of this thesis.

1.1 Surface plasmon resonance

For more than several centuries, optical properties of noble nanoparticles attracted minds of the human race. One of the famous examples of the noble nanoparticles application is the Lycurgus cup (Figure 1.1). Dichroic glass of this cup was made with the use of the gold and silver nanoparticles that gives different bright colors to the cup under different light illumination. If the light shone through the glass, the cup appears red, but if the cup is illuminated with the reflect light, then it appears green. The color of the Lycurgus cup is determined by the embedded gold and silver nanoparticles and localized surface plasmon resonance (SPR) of these particles. [1]

Electron microscopy of the dichroic glass revealed that most of the gold and silver nanoparticles embedded into the glass have spherical shape with diameters ranging from 5 to 60 nm. The shape and size of these nanoparticles will determine its localized surface plasmon resonance in the 400-600 nm range of the electromagnetic wavelengths which correspond to the color from violet to green of the visible spectrum (Figure 1.2). Furthermore, when the light shines through the Lycurgus cup, one will see only the red component of the spectrum since green and blue light is absorbed or scattered by the gold and silver nanoparticles. On the other hand if the light is reflected by the dichroic glass, the cup will appear green since the green light will be back scattered by the nanoparticles and red light will travel through the glass unperturbed.

As was shown above, the color of the cup is determined by the light interaction with plasmonic nanoparticles. When a metal particle undergos excitation due to interactions with the light, incident photons will be scattered and absorbed by the electrons of the particle lattice and will cause an enhancement of the local electromagnetic field. The collective dipolar oscillations of the free conduction electrons (plasmons) due to this excitation are called surface plasmons [2]. The photo excitation of the surface plasmons in the particles with a diameter less than the wavelength of light is denoted as a localized surface plasmon resonance [2].

For gold nanorod, the theoretical solution of absorption and scattering by cylinders with finite length is too complicated to calculate directly. Therefore, the rods are treated as very small ellipsoids. When the polarization of the incident light is parallel to different axes of the rod (ellipsoid), the absorption cross-sections are different. [3] As a result, the surface plasmon resonance is split into two parts, namely the longitudinal surface plasmon (when L_1 is used) and the transverse surface plasmon (when $L_2 = L_3$ is used). L_1, L_2, L_3 are dimensions of gold nanorod. On the other hand, the wavelength where the transverse plasmon occurs does not change with increasing aspect ratio, and occurs always around 520 nm.

Figure 1.1 The Lycurgus cup. Late Roman empire 4th Century AD. (British Museum, London)

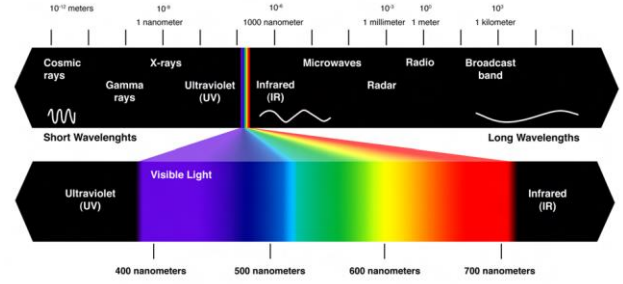

Figure 1.2 The electromagnetic spectrum. Adopted from http://blog.widen.com

1.2 Nanomaterial Overview

The word ‘nano’ comes from the Greek word ‘nanos’[4], refers to small animal or plant. In nanotechnology a particle is a unit of material which

behaves as a whole regarding chemical and physical properties [4, 5]. Particles can be divided in different categories based on their size. Particles over 2500 nm are called coarse particles while particles with the size range of 100-2500 nm are named fine particles. Particles in the size range of 1-100 nm are specifically addressed as nanoparticles.

Nanoparticles have found their way in day to day products due to their unique properties. For example titanium dioxide nanoparticles are used in the self-cleaning products [6]. Zinc oxide nanoparticles do have better UV blocking properties compared to its bulk material and that is the reason why it is used in the sunscreen lotions and textiles [7]. Clay nanoparticles are used to reinforce polymeric matrices[8]. These size-dependent properties of nanoparticles makes them favorable for many applications. Moreover, nanoparticles have size and shape dependent properties which make them totally different from bulk materials. Bulk materials have fixed properties regardless of their size but nanoparticles are totally different. For example optical properties like refractive index and absorbance of a bulk material is fixed, regardless of its mass or volume. But in nanoparticles optical properties are directly related to the size and shape of that specific nanoparticle. Another property for nanoparticles is that ratio of surface area to volume in nanoparticles is huge and usually is in the range of 106-109. Such a huge surface area gives nanoparticles unique characteristics such as optical properties and surface plasmon resonance. Gold solution does have

a goldish yellow color, but for example a solution of 20 nm gold nanospheres has red ruby color while 200 nm nanospheres has bluish color [9]. High surface area to volume ratio in nanoparticles makes diffusion of fluid faster and feasible at lower temperatures. High surface area improves physical and chemical interaction of these particles with surrounding environment which can be a solid, liquid, or polymeric matrixs. This environment can be human body and nanoparticles can be used as nanocarriers of drugs or detecting specific cells [5,9], such as, cancer cells

1.3 Gold Nanoparticles

1.3.1 Overview

Gold does have a dense and soft structure with a yellowish-goldish color. Gold as a bulk material is known for thousands years (before 3000 BC) and usually is extracted form mines [10]. It has been used widely in jewelry and decoration from ancient times. Besides its common applications, during recent decades gold has found its way in electronics and medical applications. Gold is known for its high heat and electrical conductivity while being inert and stable in most mediums.

Colloidal gold is a micro-sized or Nano-sized suspension of gold particles in a solution. Colloidal gold is known for a long time and have been vastly used in making Ruby glass back in time from fifth century [9]. Colloidal gold suspension does have very unique optical characteristics.

For example gold nanosphere suspension can have a dark, intense reddish color if the particles are less than 100 nm or purple/blue color for larger particles. Nowadays gold nanoparticles which are produced as colloidal gold, are synthesized in different shapes and sizes, according to desired application.

1.3.2 Isotropic Gold Nanoparticles

Gold nanoparticles are known to have strong absorption in the UV-visible range. Solution synthesis of isotropic gold nanoparticles is performed in a number of ways. One common route is the reduction of $HAuCl_4$ to gold ions. First used by Turkevitch in the early 1950s to produce gold nanospheres using sodium citrate as a reducing agent [11, 12], the reduction method has been adapted by numerous researchers to synthesize nanoparticles of various sizes [12]. It was initially used to synthesize isotropic nanoparticles approximately 15 nm in diameter, the procedure involves the reaction [11, 12]:

$$6AuCl_4^- + C_6H_8O_7 + 5H_2O \longrightarrow 6CO_2 + 24Cl^- + 6Au^0 + 18H^+$$

Researchers thereafter have produced nanoparticles of various sizes up to 150 nm by changing various experimental parameters such as type and concentration of reducing agent [12, 13]. The seed-mediated growth method has also been employed by many groups. In this process, gold seeds are formed first. Then a weak reducing agent such as ascorbic acid is

introduced into the solution to reduce the gold ions onto the surface of the seeds [13]. Murphy and colleagues have found that they could make gold nanospheres of controllable sizes by adjusting the seed-to-precursor ratio[12,14].

The unique optical properties of gold nanoparticles can be attributed to the principles of light scattering.The interaction of an electromagnetic field with metallic conduction band electrons produces localized oscillations of the electron clouds. Under the electric field of an incident light wave, the free electrons are displaced from the positive core. The charge difference produces a dipolar oscillation at a resonant frequency of the conduction electrons [15]. In 1908, Gustav Mie developed a model that described the absorption and scattering extinction of spherical particles by solving Maxwell's equations [16]. Because it can be applied to particles of any size, Mie's theory has been popular for solutions containing isotropic nanoparticles [12]. When electrons are confined to the surface, the localized surface plasmons contribute to the increase of field enhancement at the nanoparticle surface. This phenomenon in resonance leads to an amplification of the field in the visible range of the electromagnetic spectrum. The surface plasmon resonance is a function of a number of features, namely particle size, morphology, dielectric medium, particle interactions, and local chemical environment. Thus, for 20 nm diameter nanospheres in an aqueous solution, a strong absorption peak is seen in this

region at around 520 nm, which accounts for both the scattering and absorption [17]. The scattering process consists of the release of photons during the nanoparticle's absorption of the incident light at this resonant frequency. The simultaneous absorption takes place during the conversion of some photons into phonons (lattice vibrations). The SPR peak results in a bright red solution color of the gold nanoparticles, which renders them useful for optical applications [15, 17, 18].

In recent years, the seed-mediated growth method for nanoparticles popularized by Jana, Murphy, and others has also seen success in fabricating nanoparticles of controlled sizes. In this technique, a strong reducing agent such as sodium borohydride can be used to reduce Au^{3+} ions to gold seeds. When a weak reducing agent is introduced to the solution, Au^{3+} ions would be reduced onto the surface of the existing seeds [13]. It was shown that the morphology and size of these nanoparticles can be controlled by varying the reaction conditions.

1.3.3 Anisotropic Gold Nanoparticles

1.3.3.1 Overview

Of recent interest is the use of non-spherical or anisotropic gold nanoparticles in biomedical, optical, and sensing applications. The properties that govern their use in these applications are the plasmon absorption and changing the plamon absorption caused by shape

modification of gold nanoparticles. Given the potential applications, it becomes important to control the physical parameters of the gold nanoparticles, such as size and shape, in order to manipulate their optical properties. Shape control provides tuning over a wider range in the electromagnetic spectrum than isotropic nanoparticles. Anisotropic gold nanoparticles can absorb in the near-infrared range, which makes them valuable as photothermal agents for biological applications where, coupled with the known biocompatibility of gold, absorption by tissues in this region is minimal [19].

1.3.3.2 Gold Nanorods

Out of the anisotropic gold nanostructures, nanorods have been receiving a lot of attention for their optical properties and applications. Because Mie's theory only applies to isotropic particles, it cannot be used to model the optical behavior of nanorods. In 1912, Richard Gans modified the boundary conditions in Mie's theory for spheroids to predict the existence of two absorption bands [16]: a transverse band associated with the width of the rod and a longitudinal band related to the length of the rod [12]. For nanorods, the electric field across the particle is not uniform as observed for isotropic nanoparticles so the multipolar excitations result in more than one peak in the spectra [15].

By controlling the synthesis conditions, nanorods of different aspect ratios can be produced [17,18]. Over the years, various protocols have been

developed to produce gold nanorods. This includes porous aluminum template, electrochemical, photochemical, and seed-mediated growth methods [19]. The latter has been widely adopted in synthesizing higher aspect ratio nanorods.

1.4 Project Objectives

The main objective of this research is to design several experiments mainly for two purposes. First, based on the seed-mediate approach of making gold nanorods, find a way to optimize the seed-mediate approach and try to increase the uniformity of gold nanorods, decrease amount of byproducts during forming gold nanorods. Second, there are several mechanisms (introduce in chapter 2) trying to explain the entire forming process of gold nanorods. However, none of them is fully verified by experiments, this research is designed to find or combine an appropriate mechanism for the process of forming gold nanorods. There are many applications of gold nanorod based on its special optical properties, such as biotechnological imaging and sensing, surface-enhanced raman scattering and metamaterials, and these applications' performances can be impaired by polydispersity and low yield of gold nanorod when using seed-mediated method forms gold nanorod. Since seed-mediate approach is the most convenient and cheap method making gold nanorod, so these optimized approaches and a clearer mechanism in thesis can make this method better then improving all these applications.

1.5 Thesis Organization

This thesis is organized as follows. Chapter 2 describes theoretical background of making gold nanorods including several methods and mechanisms of forming gold naorods. Chapter 3 is devoted to describe experiments designed for first, testing the relationship between several factors and the properties of gold nanords. Second, using the experimental results try to ensure an appropriate mechanism for the process of making gold nanorods. Finally, Chapter 5 summarize work done in this thesis and lists several goals for work.

CHAPTER2
THEORETICAL BACKGROUND

This chapter aims to explain the physical and mechanistic processes involved in gold nanorod growth, as well as to outline the principles at work in the characterization methods.

2.1 Theories of Gold Nanorod Formation

2.1.1 Overview

The nanorod cannot be made by methods forming isotropic gold nanoparticles such as Turkevich method, Brust method and Perrault method, since rods are anisotropic particles. Several different methods have been used to overcome this issue. Early, some research groups used template method. Now, one of the most popular ones are synthesis in seed-mediated growth in solution [20, 21, 22]. In short, seed-mediate method is an approach which use capping agent, for example CTAB and $AgNO_3$, capping on most facets of gold nanoseeds then forcing seeds growth anisotropically and forming the rods shape nanoparticles.

2.1.2 Template Method

The template method for the synthesis of gold nanorod was first demonstrated by Martin. [23, 24] The principle of this method is the

electrochemical deposition of Au within the pores of alumina template membranes. Gold nanorods of different dimensions could be synthesized by adjusting the pore diameter of the template. [25] Gold nanorods of different lengths could be obtained through controlling the amount of gold deposited within the pores of the membrane. [26]

However, low yield is the fundamental limitation of the template method for preparing gold nanorods. [26]

2.1.3 Seed-Mediate Growth Method

The seed mediated growth method, is greatly optimized in terms of into making gold nanorod, first at 2001 by Murphy's group. [27] They used CTAB and ascorbic acid and $NaBH_4$ relatively weak reducing agents are sufficient for the seed-mediated growth mechanism and used to promote growth since the gold seeds act as a catalyst. Sodium citrate and CTAB are acting as the capping agent to force gold nanorods growth in {100} and {110} directions and facets during making process. In detail, $AuCl_4^-$ is bound to CTAB micelles followed by ascorbic acid reduction of Au^{3+} to Au^+ to form $AuCl_2$-CTAB micelles. [20,21] The growth-limiting step is the collision rate between CTAB-protected seed particles and $AuCl_2$-CTAB complexes, which in their view is faster at "tips" than at the sides and facilitates rod-shaped growth. The research group had determined that gold nanorods prepared using citrate-capped seeds and without additive Ag^+

have side faces that are Au {100} or Au {110} and have end faces that are {111} (Figure 2.1), and they rationalized that the preferential adsorption of ions to the different crystal faces of gold inhibited growth at those faces and controlled final nanoparticle shape. [22]

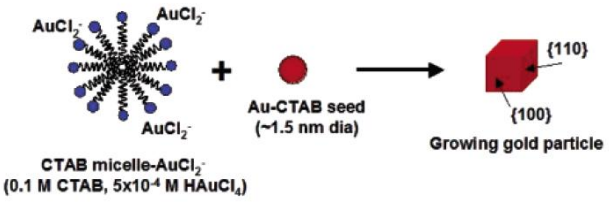

Figure 2.1. Cartoon of the mechanism of rods growth with CTAB and sodium citrate

In 2004, El-Sayed with his research group [28] did another important optimization for this seed-mediate method and increased the yield of uniform gold nanorod can up to 95%. [29] The method El-Sayed's group used to optimize is that replacing sodium citrate to silver nitrate, since $AgNO_3$ has a great ability to cap on most facets of rods such as {100} and {110} and let them growth in the specific facet {111}.

The mechanism of this improved method is still uncertain [30], there are several mechanisms explain the relationship between growth of gold nanorod and CTAB, silver nitrate. [30] Each of these proposed mechanisms has been supported by a variety of data; however, many conflicting observations have also been made, making it far from clear whether any of the proposed mechanisms should be favored over the others. Of course, it is also possible that all of the mechanisms happen during entire making process to some extent, and therefore a search for "the" mechanism may be doomed to fail.

First, the CTA−Br−Ag^+ face-specific capping agent mechanism. This theory suggests that a silver (I) bromide complex (either $AgBr_2^-$ or CTA−Br−Ag^+) acts as a face-specific capping agent, encouraging anisotropic growth in a similar mechanism to the growth of penta-twinned gold naorods. [31, 32] This mechanism assumes that the silver-bromide complex acts as a face-specific capping agent, rather than silver metal (in this respect, it is very difficult to distinguish from UPD). Recently, researchers have prepared a pure aqueous CTA−Br−Ag^+ complex and showed gold nanorod synthesis would proceed in the presence of this preformed complex. Furthermore, they found that XPS, Raman, and FTIR analysis showed that the surface chemistry of single-crystal gold nanorods was chemically identical to the CTA−Br−Ag+ complex. These data stand in contrast to the XPS/EXAFS data that has been interpreted as nearly metallic silver at the gold naorod faces. However, it should be noted that silver atoms and silver ions can be challenging to differentiate by XPS, as the spectral differences between the signals are subtle. This makes it extremely difficult to say whether face-specific capping by the silver (I) surfactant complex or silver metal is more likely. Complicating the surface analysis of these gold nanorods is the fact that metallic silver and ionic silver exist in a dynamic equilibrium under atmospheric conditions, so ex situ analysis of the products may not reveal what role silver has played during the gold nanorod synthesis.

Second mechanism, silver under-potential deposition mechanism (UPD), it is proposed that although the reduction potential of the gold naorod growth solution is not sufficient to reduce silver(I) to silver(0), there is a sufficient reduction potential to reduce silver(I) to a submonolayer of silver metal at specific faces of the gold nanorod. [33] This silver reduction at specific gold nanorod crystal faces poisons the faces and prevents further growth at these sites. UPD is thought to more difficult capping at the longitudinal facets {111} as opposed to the end-caps, and this represents a possible rationale for anisotropic growth. Increasing the concentration of silver nitrate used in the synthesis (up to a point) therefore leads to gold nanorods with increased aspect ratios and after UPD effect, CTAB ions capping over most facets of gold nanoseeds espect of {111} facets. This mechanism has been supported by XPS and EXAFS analysis of gold nanorods, which shows near-metallic Ag at or near the surface of the gold naorods, however, no analytical technique has yet been found that can show that silver is preferentially present on certain gold naorods crystal faces, rather than uniformly present all over the gold naorods surface. In addition, the formation of other anisotropic gold nanoparticles can be shown to be induced by silver UPD, so it is unclear what additional aspect of the reaction conditions would favor UPD that leads to rod growth versus the formation of other shapes. Figure 2.2 shows a schematic of each of these mechanisms. Another research group [34] agree this mechanism but

they believe the longitudinal facet is {100} facet. Figure 2.3 shows the third mechanism in this way.

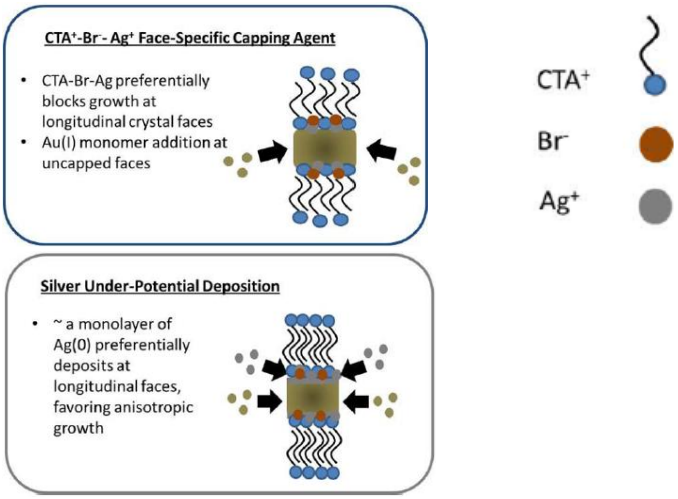

Figure 2.2. Cartoon of each mechanism of rods growth with CTAB and $AgNO_3$

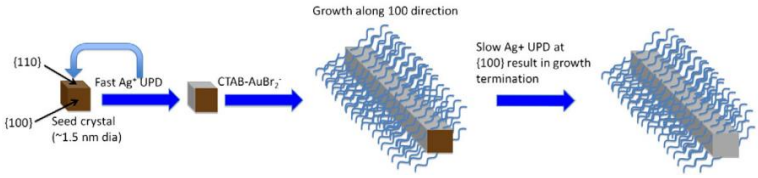

Figure 2.3. Cartoon of Underpotential deposition of silver occurs preferentially at the {110} facets of gold, leading to relatively quick growth of other facets until the slower deposition of silver on the end of the rods eventually terminates growth.

Recent years, as the improvement of experimental methods, there are several other groups using a better method and monothiolated polystyrene, PS-SH as binding agents successfully observing the whole process of gold nanorods' formation from seed to rods. [35, 36, 37, 38] Briefly, they decide the use of strongly binding polymeric ligands (monothiolated polystyrene, PS-SH) to simultaneously arrest growth and to phase transfer the particles into a nongrowth medium (toluene). Even at the earliest stages of the reaction (0−15 min), the procedure removes CTAB and unreacted precursors, while ensuring AuNR isolation as well as enabling to increase the concentration. Together, this provides a facile and reliable TEM observation. The ligand

exchange does not alter the optical spectrum of the Au NRs, and the shifts of the LSPR are simply reflective of the transfer from aqueous to organic media. So they can successfully observing the whole process of gold nanorods' formation.

In short, after observing the forming process by TEM and summarizing data from UV−vis−NIR spectra and SAXS at different time, they conclude gold nanorods' formation into 5 stages: **Stage I**, (0−2 min): seed particles with a mixture of {100} and {111} facets isotropically grow to ∼6 nm spherical nanoparticles. **Stage II**, (2−5 min): particles grow in one direction, retaining the diameter of the initial spherical. **Stage III**, (5−20 min): the growth rate of the rod length has gradually decreased while the growth rate of the diameter becomes slightly faster. The growth rate of the diameter becomes faster than the extension causing a lateral flaring of the rod leading to a dumbbell shape. **Stage IV**, (20−45 min): the overall growth significantly slows down. The growth rate of both the length and the diameter decreases. The rod sides become even and the hemispherical ends of the rods become noticeably flattened. **Stage V,** (approximately 45 min to weeks): the shape of the rod end recuperates its hemispherical shape and evolves toward a thermodynamically stable shape.

In this series experiments, the results provide insight into a number of crucial questions regarding the growth mechanism of gold nanorods. 1. Seeds growth isotopically since that seeds are too small so CTAB capping

agents cannot be absorbed on the sides of seeds. 2. The isotropic particles begin to grow anisotropically due to selective group adsorption of the CTAB agents on high energy {110}/{100} surfaces when they become comparable to the size of the agents. 3. The emergence of {250} facets of final rods is due to the process of surface reconstruction to minimize thermodynamically unfavorable {110} facets, which transform into {120} and, later, {250} facets.

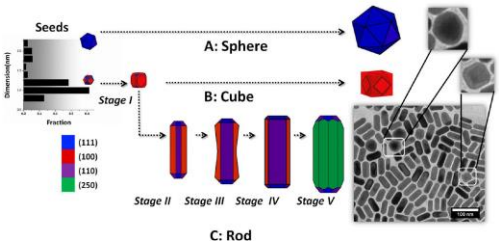

Figure 2.4 Scheme of evolution of rods, spheres, and cubes from different crystal structure seed upon the formation of a surfactant bilayer on different crystal facets at different growth stages due to a fine balance between kinetic and thermodynamic factors. The scale bar in the TEM image is 100 nm.

However, this experiment for observing the whole process of formation still cannot explain the detail of capping agents which surround the rods. So there is still uncertain that which mechanism (first or second) is right or both of them existing in rods' formation

So in this research, experiments are designed for testing which mechanism is more appropriate for gold nanorods' formation.

2.2 Optical properties of particles

2.2.1 Optical properties of noble metal particles

The optical properties of noble metal particles originate from localized surface plasmons. These phenomena occur when electromagnetic field interacts with conduction band electrons and induces the coherent oscillation of electrons. As a result, a strong absorption band appears in some region of the electromagnetic spectrum depending on the size of the particle (described in more detail in the next sub-section). [39, 40] This plasmon absorption is a small particle effect. It is absent in the individual atoms as well as in the bulk. Even for thin films, at the interface between a metal and a dielectric, the electromagnetic field can couple to the oscillations of conduction electron plasma creating surface plasmon polaritons. These surface plasmon polaritons are dispersive, propagating electromagnetic excitations on the interface that are evanescently confined in perpendicular direction. The detailed derivation and discussion of applications of surface plasmon polaritons is presented in texts like Maier [41], and is outside the scope of this article.

2.2.2 Optical properties of nano metal particles

When a metal nanoparticle is exposed to such a field, non-propagating excitations of conduction electrons create size dependent localized surface plasmons that arise simply when we consider the absorption and scattering

by gold (or other metallic) nanoparticles. When a conductor or metal is placed in an oscillating field of incoming radiation, the electrons cloud is driven into oscillations[39] (Fig. 2.5). In the case of a sub-wavelength conductive nanoparticle, the curved surface of the particle exerts an effective restoring force on these driven electrons (analogy with a damped, driven harmonic oscillator). Like any driven oscillator system, in nanoparticle case, a resonance can arise leading to the field amplification both inside and outside the particle. This resonance for gold and silver particles lies in the visible region of the electromagnetic radiation which is responsible for their bright colors in both transmitted and reflected light. The reason for field amplification as well as optical response of gold nanoparticles will perhaps more clear when approaching this problem use electrostatics. Mie [42] first explained this phenomenon theoretically by solving Maxwell's equations for a radiation field interacting with a spherical metal particle under the appropriate boundary conditions. He applied an exact electromagnetic theory for spherical particles using electrodynamics, and this describes the extinction (absorption + scattering) of spherical particles of any given size.

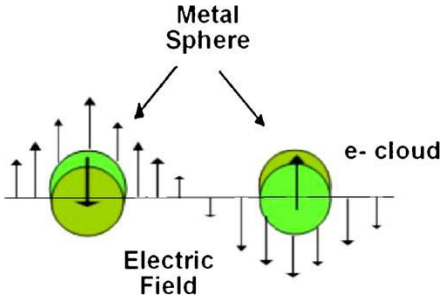

Figure 2.5 Size dependent localized plasmon resonance in nano-metal spheres.

2.2.2.1 Optical properties of gold nanosphere

For nano-metal, main part of optical properties is plasmon resonance. In the plasma model, when the electrons oscillate in response to the applied electromagnetic field, their motion is damped via collisions that occur with the frequency of 1/ γ_d. The dielectric function for free electrons of metal, can be written using Drude model as

$$\varepsilon_D(\omega) = 1 - \frac{\omega_\rho^2}{\omega^2 + i\gamma_d\omega}$$

Here the ω_ρ^2 is the plasmon frequency of free electron gas, and Since electron–electron, electron–phonon and electron-defect scattering processes determine the value of γ_d, which is a phenomenological damping constant of the bulk material, it is constant for bulk material, implying that the dielectric function is constant. [39] As we approach particle sizes comparable to the mean free path of the electrons, collisions of conduction electrons with particle surface contributes to the damping constant, as described by

$$\gamma_d(r) = \gamma_{d0} + \frac{A\nu_F}{r}$$

Here γ_{d0} is the bulk damping constant, ν_F is the velocity of the conduction electrons at Fermi energy and A includes the details of scattering process. The size dependence of damping constant makes dielectric constant and hence the resonance condition function of radius r of the particles. It may be remarked here that the consequence of this

resonantly enhanced polarization is an enhancement in the efficiency of scattering and absorption of light by metal nanoparticles.

2.2.2.2 Optical properties of gold nanorod

For gold nanorods, the plasmon absorption splits into two bands [39] (Fig. 2.6) corresponding to the oscillation of the free electrons along and perpendicular to the long axis of the rods [43]. Due to their asymmetry, [44] gold nanorods show two plasmon resonances: a longitudinal mode and a transverse mode due to electron oscillations along the major and minor axes of the particles, respectively. The transverse plasmon peak remains in the vicinity of 520 nm but the longitudinal plasmon resonance peak can be tuned to occur in the visible and the near-infrared wavelengths by changing, for example, the aspect ratio of the particles. In addition to maxima in the scattering and absorption, luminescence effects have also been observed. [45] Further, certain Raman emitting molecules adsorbed on such particles exhibit surface-enhanced Raman scattering due to the coupling of the molecules' electronic states with the plasmon resonance band. [46] To account for the optical properties of NRs, it has been common to treat them as ellipsoids, which allows the Gans formula (extension of Mie theory) to be applied. The formula [47] for randomly oriented elongated ellipsoids in the dipole approximation can be written as

$$\frac{\gamma}{N_P V} = \frac{2\pi\varepsilon_m^{3/2}}{3\lambda}\sum_{j=A}^{C}\frac{(1/P_j^2)\varepsilon^2}{\left[\varepsilon_1 + (\frac{1-P_j}{P_j})\varepsilon_m\right]^2 + \varepsilon_2^2}$$

Where Np represents the number concentration of particles, V the single particle volume, λ the wavelength of light in vacuum, and ε_m the dielectric constant of the surrounding medium and ε_1 and ε_2 are the real (n^2-k^2) and imaginary (2nk) parts of the complex dielectric function of the particles.

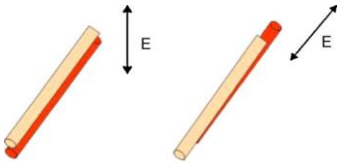

Figure 2.6. Transverse and longitudnal modes of plasmon resonance in rod-like particles.

2.3 Applications of gold nanorod

2.3.1 Introduction

The splendid optical (plasmon-related) properties of Au nanocrystals have significantly propelled their wide applications in biomedical sensing and imaging, cancer therapy, drug delivery, nanophotonics, and optoelectronics. In addition, the anisotropic plasmonic responses have provided great opportunities for Au nanorod ordered assemblies to be built up as metamaterials by exploiting their collective plasmonic responses. Such assemblies offer great potential in nanoscopic optical signal processing, manipulation, and transduction. The research works over the last two decades on the fundamental aspects of plasmonics and the development of various plasmon-based applications have opened up a new branch in nanophotonics, that is, nanoplasmonics. [48] In the following parts, I will give a brief introduction to the various applications of Au nanorods.

2.3.2 Biotechnological applications

2.3.2.1 Labelling and imaging

The scattering cross-sections of Au nanorods at their plasmon resonances can be 4–5 orders of magnitude higher than those of conventional dye molecules, [49, 50] making them excellent candidates for biomedical labelling and imaging. Besides the large light scattering capability, there are at least two other merits for employing Au nanorods as bioimaging agents. First, the synthetically tunable plasmon wavelengths of Au nanorods make them feasible for imaging with different excitation wavelengths, especially for those using near-infrared techniques. Second, the nanorods do not suffer from photobleaching as encountered with traditional dyes and semiconductor nanocrystals under the same conditions of light illumination, which makes them the most stable imaging agents.

2.3.2.2 Surface Plasmon resonance sensing

Adsorption of analytes on the surface of Au nanocrystals will change their local dielectric environment and lead to red shifts of the plasmon resonances. This refractive index change-induced plasmon shift has been widely used in the fabrication of ultrasensitive, light-weight, and remote chemical and biomedical sensors. For example, multiplex sensing of different proteins [51] and immobilizing Au nanocrystals on glass substrates for detecting hormone stanozolol. [52]

2.3.3 Plasmonic modulation of optical signals

2.3.3.1 Introduction

The nanoscale confinement of the electromagnetic field by the plasmonic resonances of metal nanocrystals allows for their integration with other nanoscale components, such as fluorophores, semiconductor nanocrystals/nanowires, and two-dimensional atomic crystals, to study the interactions of plasmons with other physical processes. [48] For gold nanorods, these interaction and the resultant phenomena are even more enriched owing to their anisotropic plasmonic properties.

2.3.3.2 Surface-enhanced Raman scattering

Due to Surface-enhanced Raman scattering significance for future chemical analysis and clinical diagnosis, tremendous efforts have been made to design and fabricate SERS substrates with strong Raman enhancements, high stability, and excellent signal uniformity, reproducibility and recyclability ever since its discovery.[48] In comparison with other nanostructures, the strong electric field enhancements and well-developed synthetic tunability of the plasmon resonances in a wide spectral range to match with excitation lasers have made Au nanorods excellent SERS substrates.

The SERS mechanism has been generally accepted to involve mainly the contributions from electromagnetic field enhancements and

chemical enhancements, with the former being dominant for excitation in resonance with the plasmon mode of metal nanostructures. Strong field enhancements at the ends of Au nanorods due to the high curvature have been demonstrated experimentally, which is consistent with the theoretical predictions. [53] The field enhancements can be further increased by bringing two nanorods close to each other. The gap region between the nanorods forms a 'hot spot' with extremely large electric field enhancements and therefore can give unprecedented SERS signals for molecules. [54, 55, 56]

In a very recent study, Kumacheva et al. have quantified the dependence of the SERS signal on the number of nanorods in a nanorod chain. [57] By controllably fabricating the different chain assemblies, they were able to correlate the ensemble-averaged SERS intensity to the number of nanorods and the extinction of the chain assemblies.

Raman spectroscopy has emerged as a promising approach for in vivo biosensing and biodetection, where Raman active molecule-coded nanomaterials are transferred to organic tissues and thereafter detected by measuring Raman scattering signals. In these applications, strong Raman signals from the coded nanomaterials are required. From this point of view, the SERS of Au nanorods is an attractive alternative for in vivo biological applications. [48, 58]

2.3.4 Metamaterials

Metamaterials are artificial materials engineered to have optical properties that cannot be found in nature. This type of materials usually mainly gains their properties from structures rather than their compositions.[59] Traditional metamaterials are usually composed of dielectric units with different spatial arrangements. They can modify the wavefronts of incident waves and redirect their propagation, giving rise to various unprecedented electromagnetic phenomena, such as negative refraction, photonic band gaps, cloaking, and electromagnetic induced transparency. [60, 61] In recent years, plasmonic metamaterials with metal nanostructures as building blocks have attracted much attention, because they are expected to work in the visible range due to the plasmon resonances of metal nanostructures. [48, 62] For example, nano-structured magnetic metamaterials.

2.3.5 Plasmon-assisted photochemical reactions

The plasmon resonances of metal nanostructures, owing to their strong light absorption capabilities, can benefit various photochemical reactions. In comparison to commonly used spherical metal nanocrystals, the much larger electric field enhancements and synthetically tunable plasmon wavelengths of Au nanorods have made them excellent alternatives for applications in photochemical reactions. [48, 63]. For example,

Misawa et al. have demonstrated plasmon-assisted water oxidation by fabricating Au nanorod arrays on the surface of TiO2 electrodes. [64]

2.3.6 Limitations of gold nanorod's optical applications

As the contents shown above, there are many optical applications of gold nanorod sue to its strong, special range of plasmon resonances, convenient, cheap making process and its tunable optical properties.(plasmon resonances) However, all these merits are based on the uninform, high yield gold nanorod making method and stable, accurate easy way to tune aspect ratio of gold nanorod.

In this thesis, experiments are designed to study the relationship between chemicals, physical factors in forming process and the size of gold nanorods, such as CTAB, $AgNO_3$ and stirring rate. In addition, thesis try to explain mechanism of formation of gold nanorods, having a better theoretical basis for researches that optimize the process of making gold nanorod in future. Last, combine all results get in thesis attempt to find a easy way to optimize the forming process. All these optimized methods can improve the performances of gold nanorod's applications and help inventing more effective applications based on the specific optical properties of gold nanorod.

2.4 Techniques in Experiments

2.4.1 Theory of UV-vis-NIR Spectrometry

Perhaps the most practical method of characterizing metallic nanoparticles is UVV is-NIR spectrometry. UV-Vis-NIR spectrometry measures the degree at which light is absorbed by a medium at different wavelengths in the ultraviolet, visible and near infrared spectra. This is done by irradiating a sample with light of known wavelength and intensity and measuring the intensity of the transmitted light. The wavelength of the light is varied by the turning of internal prisms. The machine used Varian Cary 500 Scan UV-Vis-NIR spectrophotometer In order to achieve strong intensity light over the entire UV-Vis-NIR spectrum it uses two different lamps, the first one a tungsten-halogen lamp which irradiates strongly at wavelengths in the NIR - visible spectrum and the second a twin deuterium lamp which irradiates strongly at wavelengths in the ultraviolet spectrum. The machine has slots to simultaneously measure two samples, where one is used to test the absorption spectrum of the “background” and one for the actual sample. The background is generally the medium in which the sample is suspended, toluene and water were used in this work.

2.4.2 Theory of Dynamic Light Scattering

Dynamic light scattering (DLS) is a technique which measures the light intensity reflected of particles in solution. The reflected light will change

over time as the particles undergo Brownian motion and move away from their original positions. How fast this happens depends on the hydrodynamic radius of the particles (the particles are assumed to be spherical). Therefore measurement of the rate of change of the reflected light can tell of the size of the suspended particles. The results of DLS are presented as a graph of intensity of reflected light over the size of the particles.

2.4.3 Theory of Scanning Electron Microscope

A Scanning Electron Microscope provides details surface information by tracing a sample in a raster pattern with an electron beam. The process begins with an electron gun generating a beam of energetic electrons down the column and onto a series of electromagnetic lenses. These lenses are tubes, wrapped in coil and referred to as solenoids. The coils are adjusted to focus the incident electron beam onto the sample; these adjustments cause fluctuations in the voltage, increasing/decreasing the speed in which the electrons come in contact with the specimen surface.

Controlled via computer, the SEM operator can adjust the beam to control magnification as well as determine the surface area to be scanned. The beam is focused onto the stage, where a solid sample is placed. Most samples require some preparation before being placed in the vacuum chamber.

Of the variety of different preparation processes, the two most commonly used prior to SEM analysis are sputter coating for non-conductive samples and dehydration of most biological specimens. In addition, all samples need to be able to handle the low pressure inside the vacuum chamber.

The interaction between the incident electrons and the surface of the sample is determined by the acceleration rate of incident electrons, which carry significant amounts of kinetic energy before focused onto the sample.

When the incident electrons come in contact with the sample, energetic electrons are released from the surface of the sample. The scatter patterns made by the interaction yields information on size, shape, texture and composition of the sample.

SEM produces black and white, three-dimensional images. Image magnification can be up to 10 nanometers and, although it is not as powerful as its TEM counterpart, the intense interactions that take place on the surface of the specimen provide a greater depth of view, higher resolution and, ultimately, a more detailed surface picture.

CHAPTER 3
SYTHENSIS AND CHARACTERISTICAL OF GOLD NANOROD

3.1 Introduction

This part is about using seed-mediate method making gold nanorod and studying how CTAB, $AgNO_3$, stirring rate, pH value and so on impact the growth of gold nanorods. Second, this part is designed to use ultraviolet–visible spectroscopy test rods' surface plasmon resonance and based on these data and image trying to verify which mechanism that be posted to explain the process of forming gold nanorods is right. Last, this part will also learn the relationship between size of seeds and growth of gold nanorods.

3.2 Material

Most of materials are purchased from Sigma-Aldrich Inc. and are used as received. These include $HAuCl_4+3H_2O$ or Gold Chloride Trihydrate (99.9+ % (Catalogue No. 520918-1G)); $AgNO_3$ or Silver Nitrate (99.9999% Metals Basis (Catalogue No. 204390-10G)); CTAB or Hexadecyltrimethylammonium Bromide (Biox Catalogue No. h9151-25G); L-Ascorbic acid (Bioultra, ≥ 99.5 % RT (catalogue No. 95209-50G)); $NaBH_4$ or Sodium Borohydride (Granules, 99.99 % ME (Catalogue No.

480886-25G)). HCl and NaOH are purchased from Fisher Scientific and are used as received. HCl (0.1Mol Hydrochloric Acid (Catalogue No. A144S-212)). NaOH (50% w/w Sodium Hydroxide Bioxtra (Catalogue No. SS254-4)). DI water was used for glassware washing and preparing solutions. A Millipore UV-synergy water purification system was used to produce the DI water. The structures of the main reagents are shown below.

CTAB:

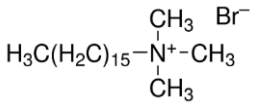

Figure 3.1a CTAB structure

$HAuCl_4+3H_2O$:

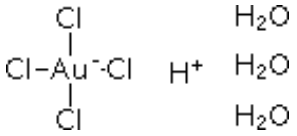

Figure 3.1b $HAuCl_4+3H_2O$ structure

$AgNO_3$:

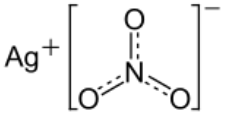

Figure 3.1c $AgNO_3$ structure

L-Ascorbic Acid:

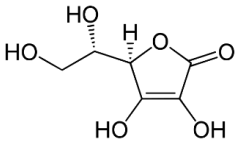

Figure 3.1d L-Ascorbic Acid structure

$NaBH_4$:

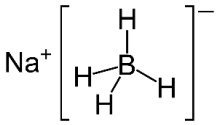

Figure 3.1e $NaBH_4$ structure

3.3 Instrumentation

Absorption spectra are primarily obtained using a Varian Cary 500 Scan UV-Vis-NIR spectrophotometer unless otherwise indicate. Scanning

electron microscope (SEM) is performed using a FEI Magellan 400 XHR SEM. Centrifugation is done using a Thermo Scientific Legend 14 Centrifuge Model No. 11210807. Dynamic light scattering (DLS) tests are done using Malvern Zetasizer Nano DLS machine.

3.4 Standard Seed-Mediate Method

3.4.1 Proposal of the standard seed–mediated method

Because the standard method is the basic method for this paper, so it is necessary to found an optimized seed-mediate method. By reading several papers [65, 66, 67, 68, 69], I decide use this seed-mediate method as the standard method.

Step-1 Preparation of Gold Seed

A seed solution containing gold seeds are made at step one. First, a centrifuge tube is placed inside the warm water bath water bath temperature is kept at 28 centigrade. 0.250 mL of 0.010 M $HAuCl_4$ solution is mixed with 10.0 mL of 0.100 M CTAB under vigorous stirring in the centrifuge tube (600 rpm). Immediately, this solution is reduced with 600 μL of freshly made, ice-cold 0.010 M sodium borohydride ($NaBH_4$) and is vigorously stirred (700rpm) for 10 min to ensure that all excess of $NaBH_4$ have volatilized

Step-2 Synthesis of Gold Nanorod

In a typical experiment, a vial is placed inside the warm water bath and temperature of water bath is kept at 28 centigrade. 5.00 mL of 0.100 M CTAB, 0.250 mL of 0.010 M $HAuCl_4$, and 0.030 mL of 0.010 M $AgNO_3$ solutions are added in that order, one by one, to the centrifuge tube, followed by gentle mixing by inversion. The solution at this stage appears bright brown-yellow in color. Then after one minute, 0.040 mL of 0.100 M L-Ascorbic acid (AA) is added to it. The solution becomes colorless upon addition and mixing of ascorbic acid. Finally, 0.050 mL of seed solution (described in step 1) is added, after gentle mixing for several seconds the solution should be kept undisturbed for at least 12 hours before testing.

Details of making all chemical solutions

In this experiment, the 0.010 M $HAuCl_4$ solution is made by adding 0.0680 g of $HAuCl_4$ to 20.0 mL of DI water. 0.100 M CTAB solution is made by adding 0.583 g of CTAB to 16.0 mL of DI water (The aqueous CTAB solution need to be putted in 40 centigrade water bath overnight in order to allow a complete dissolution of the surfactant). The 0.100 M $NaBH_4$ solution is made by adding 0.0946 g of $NaBH_4$ to 25.0mL of DI water that have been cooled in an ice bath. 1.00 mL of this 0.100 M $NaBH_4$ solution is added to 9.00 mL of ice-cold DI water to create the final 0.010 M $NaBH_4$ solution. 0.010 M $AgNO_3$ solution is made by adding 0.0340 g

of $AgNO_3$ to 20.0 mL of DI water and this solution must be made in dark. At last, the 0.100 M L-Ascorbic acid (AA) solution is made by adding 0.176 g of AA to 10.0 mL of DI water and this solution must be fresh.

3.4.2 Result and Discussion

Since the optical spectra of the plasmons are very informative if spectra are taken in aqueous solution with a standard spectrophotometer. [65] (The position of the plasmon band is well-known to be sensitive to the local dielectric constant of the media, and the aggregation state of the particles; the nanoparticles are well-dispersed in the same DI water for testing and comparison can be ensured in all experiments.) Nanorods show two plasmon bands, commonly ascribed to light absorption (and scattering) along both the longitudinal axis and the transverse axis (absorption and scattering will cause surface plasmon resonance) of the colloidal particles. [65] So doing an optical plasmon resonance test (ultraviolet–visible spectroscopy) can test properties of gold nanorods.

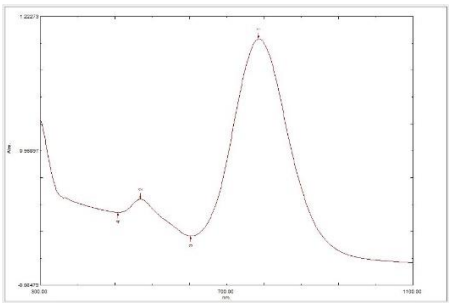

Figure 3.2 Ultraviolet–visible spectrum of gold nanorod made by standard method

Table 3.1. Resonances of the longitudinal and transverse surface plasmons for gold nanorod

	Surface Plasmon Resonance (nm)	Abs.
Longitudinal axis	768	1.11
Transverse axis	515	0.334

Figure 3.3 Picture of gold nanorod made by standard seed mediate-method

Based on the ultraviolet–visible spectra, there are only two peaks (longitudinal and transverse peaks) show on the spectra and without extra peaks. This verifies that the gold nanorods made by standard seed-mediate approach are in good monodisperse state and most of them are uniform in one size. Therefore this method can be used as control group for next several experiments and it shows that the color of rods with the surface plasmon resonance about 770nm is light purple.

3.5 The Influence of Factors to Gold Nanorod

3.5.1 Introduction

The mechanism of forming gold nanorods in the chapter 2 shows that the CTAB, $AgNO_3$ and gold nanoseed are three main factors to impact growth of gold nanorod. So in this part experiments will be designed to show how these factors impact the growth and verify the mechanism mentioned in part two, also try to find a way to optimize the uniformity of gold nanorods made by seed-mediate approach.

3.5.2 Variation Concentration of CTAB

3.5.2.1 Experimental Design

This experiment will test the relationship between CTAB concentration and size distribution of gold nanorod. In this part, more work will be focus on learning how the size distribution change when decreasing concentration of CTAB rather than increasing it. The method is as follow.

Step-1 Preparation of Gold Seed

This step is same as the standard seed-mediate growth method.

Step-2 Synthesis of Gold Nanorod

First, 9 vials, named as 1 to 9 are placed inside the warm water bath and temperature of water bath is kept at 28 centigrade. 1.00 to 5.00 mL (increasing 0.500 ml of CTAB per one set) of 0.100 M CTAB, 0.250 mL of 0.010 M $HAuCl_4$, and 0.030 mL of 0.010 M $AgNO_3$ solutions are added in that order, one by one, to 9 vials respectively and No.9 set is control group (red word shown in table), followed by gentle mixing by inversion. After one minute, 0.040 mL of 0.100 M L-Ascorbic acid (AA) are added to them. The color of solutions changed from dark yellow to colorless. Finally, 0.050 mL of seed solution (described in step 1) is added to each tube to initiate the growth, after gentle mixing for several seconds the solution should be kept undisturbed in warm water bath for at least 12 hours before testing.

The gold naorod solution is kept in water bath undisturbedly for 5 days to let rods fully growth and then tested by ultraviolet–visible spectroscopy

3.5.2.2 Result and Discussion

Table 3.2 Ultraviolet–visible spectra data for gold nanorods with different amount of CTAB

Volume of CTAB (mL)	1	1.5	2	2.5	3	3.5	4	4.5	5
Surface Plasmon Resonance of Longitudinal Axis (nm)	699	726	740	750	758	761	766	766	775
Surface Plasmon Resonance of gold nanoparticles (nm)	550	554	568	567	564	558	566	560	/
Surface Plasmon Resonance of Transverse Axis (nm)	528	524	524	524	520	521	518	517	516
Absorbance of Longitudinal Axis resonance	0.713	0.775	0.607	0.575	0.580	0.577	0.528	0.517	0.483
Absorbance of Gold Nanoparticles resonance	0.424	0.365	0.295	0.262	0.234	0.213	0.153	0.132	/
Absorbance of Transverse Axis Resonance	0.457	0.373	0.283	0.250	0.232	0.224	0.177	0.167	0.169
Absorbance Ratio of Nanoparticles to Longitudinal Axis of Rod	0.595	0.486	0.466	0.456	0.403	0.388	0.290	0.255	/

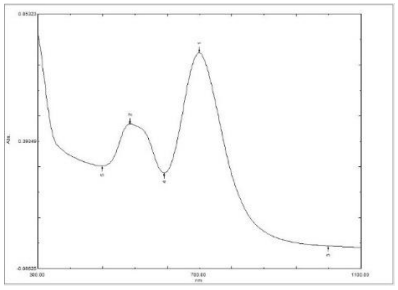

Figure 3.4a uv spectrum of AuNR made by 1mL CTAB

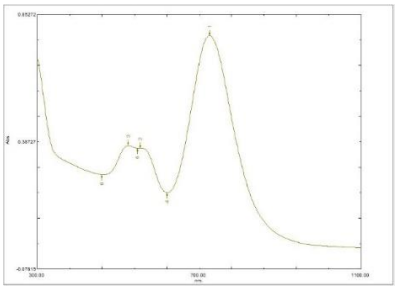

Figure 3.4b uv spectrum of AuNR made by 1.5mL CTAB

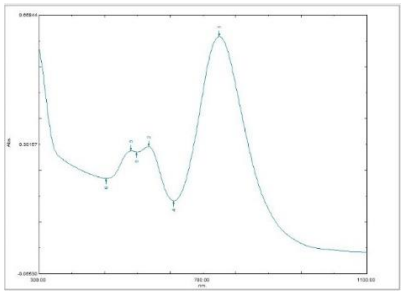

Figure 3.4c uv spectrum of AuNR made by 2mL CTAB

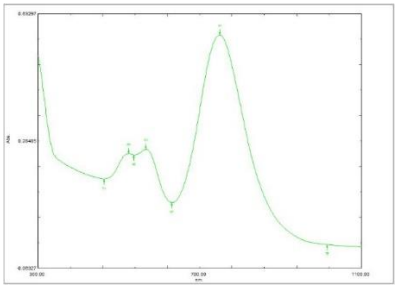

Figure 3.4d uv spectrum of AuNR made by 2.5mL CTAB

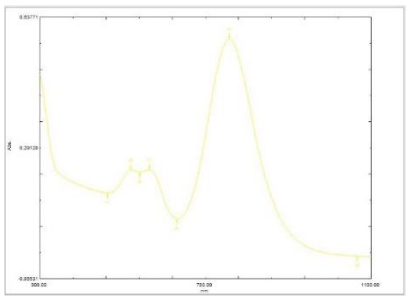

Figure 3.4e uv spectrum of AuNR made by 3mL CTAB

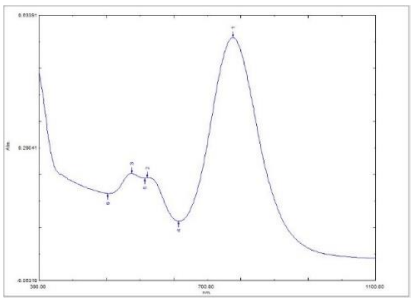

Figure 3.4f uv spectrum of AuNR made by 3.5mL CTAB

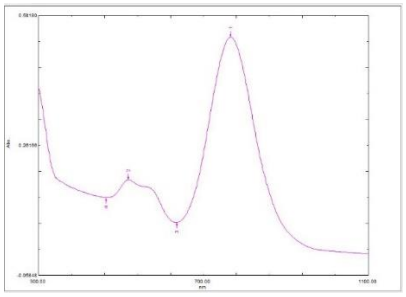

Figure 3.4g uv spectrum of AuNR made by 4mL CTAB

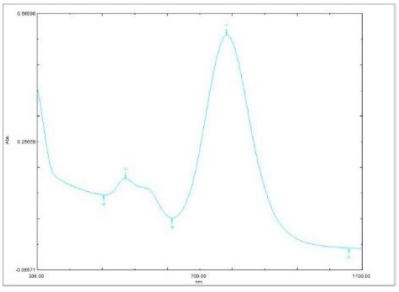

Figure 3.4h uv spectrum of AuNR made by 4.5mL CTAB

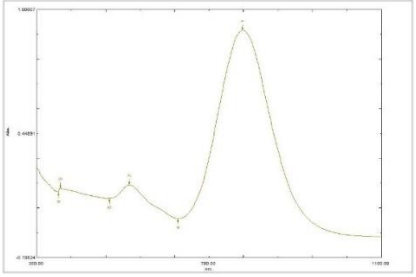

Figure 3.4i uv spectrum of AuNR made by 5mL CTAB

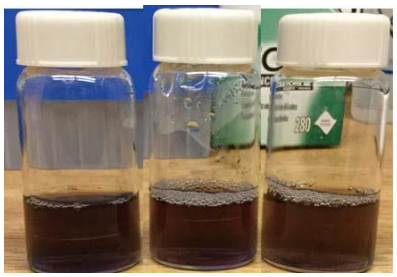

Figure 3.5 AuNR with CTAB increase from left to right

The change of concentration is from 0.0925 M (control group 5mL) to 0.0714M (1mL CTAB). As the concentration decreasing several changes appear in gold nanorod solution. First, there are some gold nanoparticles in other shapes appearing during formation of gold nanorod. Since the resonance of nanoparticles is not apparent distinguished from the transverse resonance in uv-vis spectra, so main part of this byproducts are nanoparticles with similar diameter and close to the size of transverse axis of gold nanorods. Second, the longitudinal surface plasmon resonance has a left change as concentration of CTAB decreasing. Murphy and his research group has found that [65] as the aspect ratio increases, the position of the longitudinal plasmon band red-shifts, and the transverse plasmon band position stays relatively constant at ~520 nm. Compared with Murphy's result the left shift means aspect ratio decreases and rods becomes shorter. Third, the absorbance ratio of byproducts' resonance to longitudinal axis resonance increasing as the concentration of CTAB decreasing. Last, figure 3.4 shows color of gold solution changing from light purple to dark purple when decreasing the concentration of CTAB, this shows that change in aspect ratio can be seen with the naked eye.

Last, several things must be concerned. First, absorbance can be only used in each uv-vis spectra and cannot be compared between different uv-vis spectra, because the fusion of two neighborhood gold nanorods [70] happen during the 5 days before testing, and since the rods will lose their

unstable tips during the first several days so although knowing the fusion between rods, waiting several days before testing cannot be canceled. The absorbance of each longitudinal axis resonance is different with each other since the fusion happens randomly.

3.5.3 Variation Concentration of $AgNO_3$

3.5.3.1 Experimental Design

Based on the mechanism mentioned in theoretical background, $AgNO_3$ can make a great contribution on controlling the aspect ratio of gold nanorod. In this experiment there are mainly two purposes. First, test this rule between $AgNO_3$ and gold nanorod. Second, make sure this tendency is monotonous or periodical variation.

Step-1 Preparation of Gold Seed

This step is same as the standard seed-mediate growth method.

Step-2 Synthesis of Gold Nanorod

First, 11 vials named from 1 to 11 are placed inside the warm water bath and temperature of water bath is kept at 28 centigrade. 5.00 mL of 0.100 M CTAB, 0.250 mL of 0.010 M $HAuCl_4$, and 0-0.100 mL of 0.010 M $AgNO_3$ (increasing 0.010 mL of $AgNO_3$ per set) solutions are added in this order respectively one by one, to the vials, and No.4 set is the control group (red word shown in table), followed by gentle mixing by inversion. After one minute, 0.040 mL of 0.100 M L-Ascorbic acid (AA) are added

to them. The color of solutions changed from dark yellow to colorless. Finally, 0.050 mL of seed solution (described in step 1) is added to each tube to initiate the growth, after gentle mixing for several seconds the solution should be kept undisturbed in warm water bath for at least 12 hours before testing.

The gold nanorod solution is kept in water bath undisturbedly for 5 days to let rods fully stable and then tested by ultraviolet–visible spectroscopy.

3.5.3.2 Result and Discussion

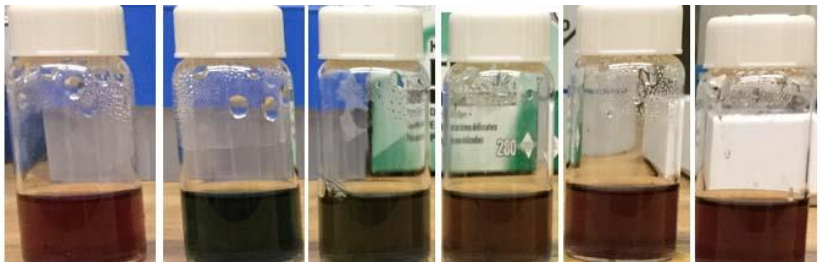

Figure 3.6 Picture of gold nanorods growth with different amount of $AgNO_3$ amount increase from left to right

Table 3.3 Ultraviolet–visible spectra data for gold nanorods with different amount of $AgNO_3$

Volume of $AgNO_3$ (mL)	0	10	20	30	40	50	60	70	80	90	100
Surface Plasmon Resonance of Longitudinal Axis (nm)	/	671	729	768	778	764	766	754	746	745	739
Surface Plasmon Resonance of gold nanoparticles (nm)	529	/	/	/	565	560	557	558	552	558	554
Surface Plasmon Resonance of Transverse Axis (nm)	/	515	514	513	515	515	517	518	526	525	524
Absorbance of Longitudinal Axis resonance	/	0.555	0.777	0.819	0.861	0.815	0.838	0.672	0.519	0.475	0.435
Absorbance of Gold Nanoparticles resonance	0.381	/	/	/	0.201	0.216	0.228	0.257	0.241	0.262	0.259
Absorbance of Transverse Axis Resonance	/	0.244	0.236	0.251	0.261	0.250	0.246	0.257	0.239	0.238	0.240
Absorbance Ratio of Nanoparticles to Longitudinal Axis of Rod	/	/	/	/	0.233	0.265	0.272	0.381	0.465	0.551	0.596

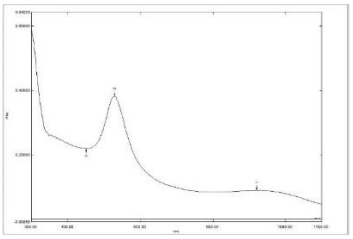

Figure 3.7a uv spectrum of AuNR made by 0mL $AgNO_3$

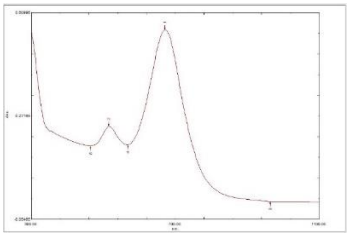

Figure 3.7b uv spectrum of AuNR made by 10mL $AgNO_3$

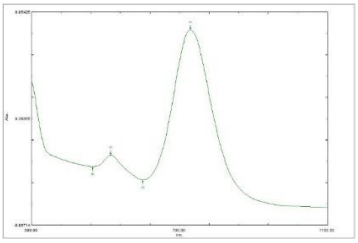

Figure 3.7c uv spectrum of AuNR made by 20mL $AgNO_3$

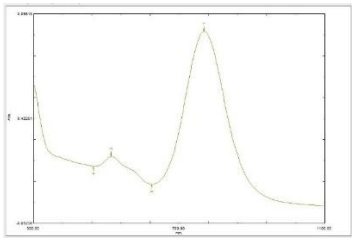

Figure 3.7d uv spectrum of AuNR made by 30mL $AgNO_3$

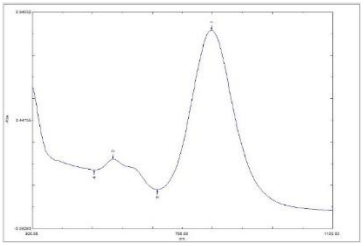

Figure 3.7e uv spectrum of AuNR made by 40mL $AgNO_3$

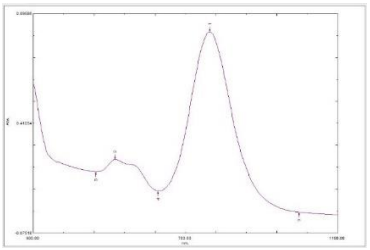

Figure 3.7f uv spectrum of AuNR made by 50mL $AgNO_3$

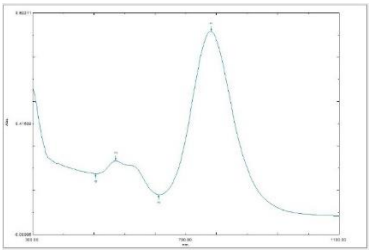

Figure 3.7g uv spectrum of AuNR made by 60mL $AgNO_3$

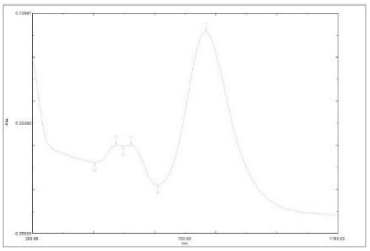

Figure 3.7h uv spectrum of AuNR made by 70mL $AgNO_3$

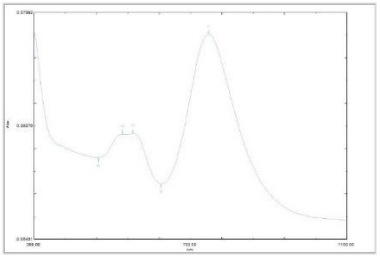

Figure 3.7i uv spectrum of AuNR made by 80mL $AgNO_3$

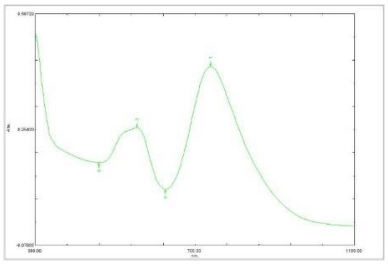

Figure 3.7j uv spectrum of AuNR made by 90mL $AgNO_3$

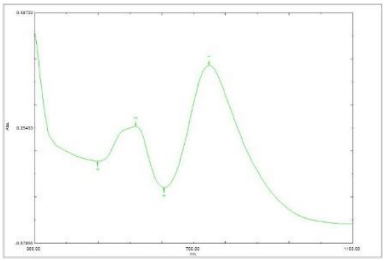

Figure 3.7k uv spectrum of AuNR made by 100mL $AgNO_3$

The concentration of $AgNO_3$ changes from 0 to 0.185M (volume changes from 0 to 100μL and 30μL is control group). Compared with the relationship between gold nanorod and concentration of CTAB, the relationship between rod and concentration of $AgNO_3$ is more complicated. Same as CTAb experiments, absorbance of surface plasmon resonance from different uv-vis spectrum cannot be compared since randomly fusion between neighborhood rods.

First, when there aren't any $AgNO_3$ in gold solution, rod shape cannot be formed and only a small part of gold atoms aggregate with seeds forming gold nanosphere, as slowing increasing the amount of $AgNO_3$ up to the 30.0μL (30μL is the control group the concentration is 5.56×10^{-2} M) it can help gold nanoseed doing an anisotropic growth forming rod in this part as amount of $AgNO_3$ increasing, length of rods becomes longer and during whole process no byproducts being formed. So for growth solution the commonly used 2.30×10^{-6} M gold nanoseed and 0.100 M CTAB,1.852×10^{-2} M to 5.56×10^{-2} M of $AgNO_3$ are the best choice to make different aspect ratio of gold nanords.

Keep increasing the amount of $AgNO_3$ to 40.0μL the length of gold naorod can increase a little but since excess of $AgNO_3$ being add, a little amount of byproducts appear these byproducts are similar with the ones appear in CTAB experiment having small range of size and similar with the size of transverse axis of rods. Since the amount of byproduct is very

small so uv-vis spectra cannot figure out a resonance peak for them. (The peak and absorbance shows in table is estimated by Windows Excel)

Adding more $AgNO_3$ up to 60.0μL, twice as much as concentration of control group adding, rods are no longer lengthen by increasing $AgNO_3$ and keep similar length with control group, meanwhile, amount of byproducts increasing a lot. (The peak and absorbance of byproducts shown in table is estimated by Windows Excel)

Next, as the amount of $AgNO_3$ keep increasing up to 80.0μL, length of gold nanorod decrease and amount of byproducts increase a lot so the uv-vis spectroscopy can show a plasmon resonance peak for them.

Last, keep adding $AgNO_3$ to 100μL since great excess of $AgNO_3$, there are a large amount of byproducts in rod solution forming a size distribution near transverse axis of gold nanorod and result in uv-vis spectroscopy cannot figure out the plasmon resonance of transverse axis. So only longitudinal and byproduct's plasmon resonance peak show in result images. (The peak and absorbance of transverse axis shown in table is estimated by Windows Excel)

Figure 3.5 is the image of gold nanorods made by different amount of $AgNO_3$ (from left to right are 0, 10, 20, 30, 90, 100μL). It shows that first, without $AgNO_3$, gold naonsphere which surface plasmon resonance is about 530nm, the color is pink-purple. Second, when adding $AgNO_3$ solution begins forming rods instead of sphere. The color of rods is green

when surface plasmon resonance of longitudinal axis is 670nm, is dark green when plasmon resonance is 730, is light purple when plasmon resonance is 770nm. It is also shows the last two sets (90,100μL $AgNO_3$) when plasmon resonance changes from 770 to 740 color of them still similar with the 770 set. Because this two group have a large of gold nanoparticles with other shape, so the color change cannot show the resonance change clearly.

Based on data and image from uv-vis spectroscopy, the relationship between $AgNO_3$ and growth of gold nanorod is like this. First, $AgNO_3$ is one of the necessary chemicals for gold seed forming gold nanorods in the situation that using a small amount of CTAB. Second, although $AgNO_3$ is necessary for rods, when it is over does, it results in forming byproducts and shorten gold nanorods. The amount of byproducts and the length shorten by $AgNO_3$ are positive correlation with extra amount of $AgNO_3$

3.5.4 Variation Stirring Rate

3.5.4.1 Experimental Design

Based on the experience of making gold nanorods, changing the stirring rate at second step will affect the aspect ratio and size distribution of gold nanorods. This experiment is designed as study this relationship systematically and ensure it is positive correlation or negative correlation.

Step-1 Preparation of Gold Seed

This step is same as the standard seed-mediate growth method.

Step-2 Synthesis of Gold Nanorod

First, four vials named as a, b, c, d, are placed inside the warm water bath and temperature of water bath is kept at 28 centigrade. 5.00 mL of 0.100M CTAB, 0.250 mL of 0.010 M $HAuCl_4$, 0.030 mL of 0.010 M $AgNO_3$ solutions are added in all tubes followed by gentle mixing by inversion. After one minute, 0.040 mL of 0.100 M L-Ascorbic acid (AA) are added to them. The color of solutions changed from dark yellow to colorless. Finally, 0.050 mL of seed solution (described in step 1) is added to each tube to initiate the growth, The solutions in vials a, b, c, d should be kept under stirring rate 0 rpm, 80rpm, 400rpm, 600rpm respectively for 5 hours. Vial a is the control group. After stirring for 5 hours, solution should be kept undisturbed in warm water bath for at least 12 hours before testing.

The gold nanorod solution is kept in water bath undisturbedly for 5 days to let rods fully stable and then tested by ultraviolet–visible spectroscopy.

3.5.4.2 Result and Discussion

Table 3.4 Ultraviolet–visible spectra data for gold nanorods with different stirring rate

Stirring Rate (rpm)	0	80	400	600
Surface Plasmon Resonance of Longitudinal Axis (nm)	769	769	768	791
Surface Plasmon Resonance of gold nanoparticles (nm)	/	555	560	591
Surface Plasmon Resonance of Transverse Axis (nm)	518	519	514	517
Absorbance of Longitudinal Axis resonance	0.990	0.843	0.934	0.828
Absorbance of Gold Nanoparticles resonance	/	0.213	0.241	0.191
Absorbance of Transverse Axis Resonance	0.315	0.260	0.268	0.219
Absorbance Ratio of Nanoparticles to Longitudinal Axis of Rod	/	0.252	0.257	0.231

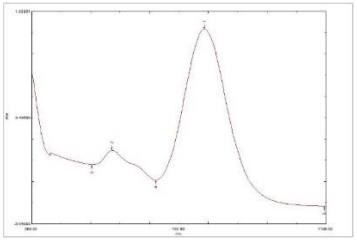

Figure 3.8a uv spectrum of AuNR made without stirring

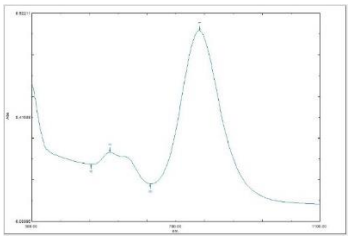

Figure 3.78 uv spectrum of AuNR made under 80rpm stirring

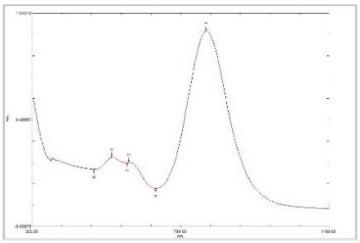

Figure 3.8c uv spectrum of AuNR made under 400rpm stirring

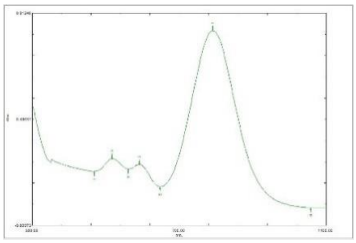

Figure 3.8d uv spectrum of AuNR made under 600rpm stirring

Because these four gold sample are hard to distinguish by naked eyes, so there are no images in result and discussion part.

From ultraviolet–visible spectra and absorbance data, the relationship between stirring rate and growth of gold nanorods is that adding stirring step at the last during making gold nanorods result in forming more byproducts than the group which doesn't include stirring step. However there aren't any detail rules between these two things.

When gold solution is under stirring situation, the chance of rods contacting each other highly increase, so fusion effect happens more often than control group. A part of fusion particles have a diameter larger than transverse axis of rods but smaller than longitudinal axis, so spectra can show this part of fusion gold nanoparticles and fusion effect is a randomly process so this is experiment can only find a rough relationship between stirring rate and gold nanorods' growth.

3.5.5 Variation Size Distribution of Seed

3.5.5.1 Experimental Design

Except CTAB, $AgNO_3$, these two factors impact the growth of gold nanorods at second step, gold seed another important factor to rods' growth, the relationship between its properties and rods' growth should also be studied.

The size of seed should be kept small by setting an appropriate stirring rate in the standard method. However, if change the stirring rate during first step then size will become larger than usual. This experiment's goal is to study how this larger size of seeds affect the growth of gold nanorod.

Step-1 Preparation of Gold Seed

First, five vials named a, b, c, d, e are placed inside the warm water bath water bath temperature is kept at 28 centigrade. 0.250 mL of 0.010 M $HAuCl_4$ solution is mixed with 10.0 mL of 0.100 M CTAB in each tube and under vigorous stirring (600 rpm). Immediately, all solution are reduced with 600μL of freshly made, ice-cold 0.010 M sodium borohydride ($NaBH_4$) and these seed solutions in vials are vigorously stirred by different rate 900 rpm, 700 rpm, 350 rpm, 0 rpm, respectively for 15 min after all additions have been made without capping and ensure that all excess of $NaBH_4$ have volatilized. Group d is the control group.

Step-2 Synthesis of Gold Nanorod

This step is same as the standard seed-mediate growth method.

3.5.5.2 Result and Discussion

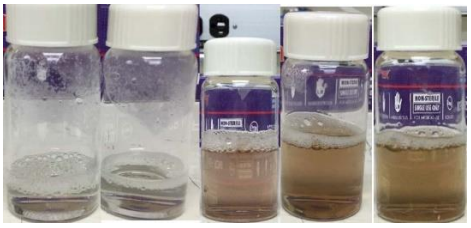

Figure 3.9 Gold nanoseed growth with 0,200,500,700,900rpm stirring (from left to right)

Figure 3.10 Gold nanorod growth with different kinds of seeds

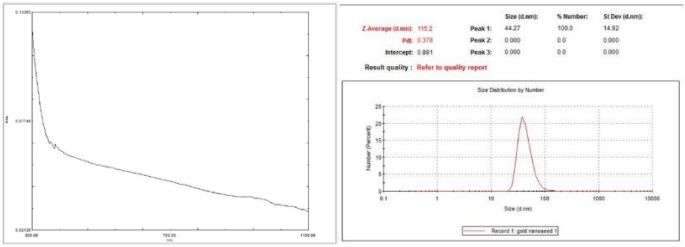

Figure 3.11a uv-vis spectrum (left) and DLS data for rods growth with seed under 0rpm stirring rate

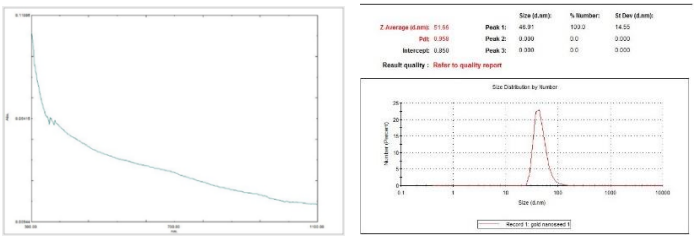

Figure 3.11b uv-vis spectrum (left) and DLS data for rods growth with seed under 200rpm stirring rate

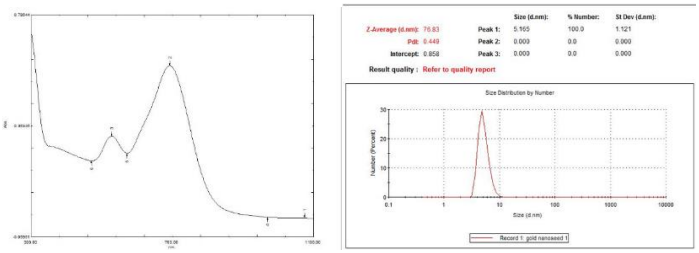

Figure 3.11c uv-vis spectrum (left) and DLS data for rods growth with seed under 500rpm stirring rate

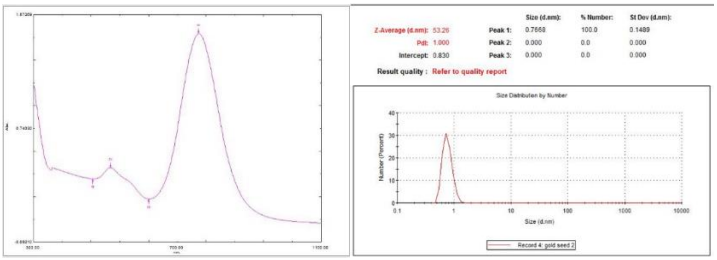

Figure 3.11d uv-vis spectrum (left) and DLS data for rods growth with seed under 700rpm stirring rate

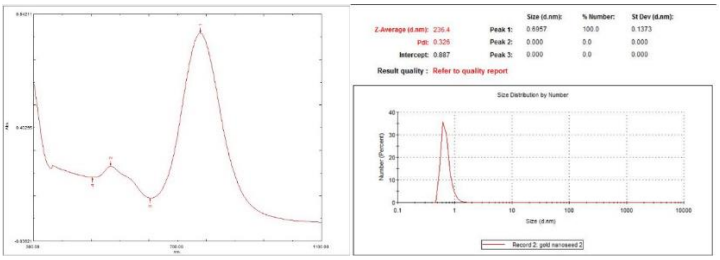

Figure 3.11e uv-vis spectrum (left) and DLS data for rods growth with seed under 900rpm stirring rate

Table 3.5 DLS and Ultraviolet–visible spectra data of gold nanorods and seeds

Stirring Rate (rpm)	0	200	500	700	900
DLS data of seeds (nm)	44.3	46.9	5.17	0.767	0.696
Surface Plasmon Resonance of Longitudinal Axis (nm)	/	/	692	759	763
Surface Plasmon Resonance of Transverse Axis (nm)	/	/	528	514	514
Absorbance of Longitudinal Axis resonance	/	/	0.593	1.43	0.769
Absorbance of Transverse Axis Resonance	/	/	0.324	0.453	0.254

Based on all these data and images, several result can be shown. First, as there are no stir or slow stir rate during seed forming process, then there aren't any rods can form from this seed solution, instead of seed, a large number of nanoparticles which are much bigger than seed formed, the colorless color of seed solution under 0 and 200rpm stirring rate and their DLS data can prove this.

Second, when the stirring rate achieve the minimum amount to form the gold nanoseed, it is apparent that as the stirring rate higher, the size of seed becomes smaller. The images and DLS data of gold nanoseed under 500,700,900 rpm stirring rate verify this.

Third, as the seed become smaller, the rods become longer. The uv-vis spectra of gold nanorod forming by seeds under 500,700,900 rpm stirring rate can prove this.

Last, color of seed solution is pink as the size of seed is about 5nm, when it turns to less than 1nm, the color is brown and difficult to

distinguish each other by color. For gold nanorods, its color is dark blue when its surface plasmon resonance of longitudinal axis is about 700nm, and its color is light purple when plasmon resonance is 760 to 770nm.

All this properties show that a high stirring rate during making gold nanoseed is necessary otherwise there aren't any seed form from the solution, since first the high rate stirring can separate Au ions or atoms from each other letting them form into seeds instead of big gold aggregates . Second, in this step BH_4^- ions reduce $AuCl_4^-$ into Au atom but BH_4^- ions are easily oxidize by O_2, so it is necessary making BH_4^- ions react with $AuCl_4^-$ ions as quick as possible, highly speed stirring can make these two ions contact and react faster than no stir group. So stir seed solution in high speed is necessary for forming nanoseeds. Methods which want to optimize the process of seed formation, the chemicals being used must be stable under high rate stirring for at least 1 hour.

Another conclusion shown in this experiment is that if there isn't any seed in gold solution, this solution cannot form any rods or byproducts that have a surface plasmon resonance in 300nm to 1100nm.

3.5.6 Variation pH Value

3.5.6.1 Experimental Design

Beside the chemicals and seed, another important factor which can impact the growth of gold nanorod is the pH value of the solution rods

growth in. Based on several papers [66, 69, 70, 71, 72, 73, 34], the pH value of the growth solution (step-2) can affect the shape of gold nanorod and increase their aspect ratio. So the experiment in this part is designed to, first, test the influence of pH value and try to learn more detail relationship between aspect ratio of gold nanorod and pH value of the growth solution. Second try to find if changing pH value of solution can optimize the standard seed-mediate approach. Since using standard method make gold nanorod, there are still a very small amount of byproducts forming, although uv-vis machine cannot figure them out.

Step-1 Preparation of Gold Seed

This step is same as the standard seed-mediate growth method.

Step-2 Synthesis of Gold Nanorod

First, eight vials, named as a, b, c, d, e, f, g, h are placed inside the warm water bath and temperature of water bath is kept at 28 centigrade. 5.00 mL of 0.100 M CTAB, 0.250 mL of 0.010 M $HAuCl_4$, and 0.030 mL of 0.01 M $AgNO_3$ solutions are added in that order, one by one, to each of the centrifuge tubes, followed by gentle mixing by inversion. After one minute, 0.040 mL of 0.100 M L-Ascorbic acid (AA) is added to it. The color of solutions changed from dark yellow to colorless. Then 0.025 mL, 0.050 and 0.100 mL 50%w/w NaOH are added to tube a, b and c respectively. Vial d is kept without adding any hydrochloric acid or sodium

hydroxide. 0.015, 025, 0.050 and 0.100 mL, 0.015 M HCl were injected into tube e, f, g and h respectively. Finally, 0.050 mL of seed solution (described in step 1) is added to each vial to initiate the growth, and the solution should be kept under 80rpm stirring in warm water bath for at least 12 hours before testing.

The gold nanorod solution is kept in water bath undisturbedly for 5 days to let rods fully stable and then tested by ultraviolet–visible spectroscopy.

3.5.6.2 Result and Discussion

Table 3.6 pH value and Ultraviolet–visible spectra of each gold solution

Volume of chemicals	0.025mL NaOH	0.050mL NaOH	0.100mL NaOH	0mL NaOH or HCL	0.015mL HCl	0.025mL HCl	0.050mL HCl	0.100mL HCl
Calculative pH value	12.45	12.42	13.15	4.68	2.45	2.23	2.13	1.74
Measuring pH value	12.32	12.65	13.06	4.6	2.51	2.31	2.05	1.83
Volume of chemicals	0.025mL NaOH	0.050mL NaOH	0.100mL NaOH	0mL NaOH or HCL	0.015mL HCl	0.025mL HCl	0.050mL HCl	0.100mL HCl
Surface Plasmon Resonance of Longitudinal Axis (nm)	/	/	/	776	778	846	902	965
Surface Plasmon Resonance of Transverse Axis (nm)	/	/	/	518	511	517	521	525
Absorbance of Longitudinal Axis resonance	/	/	/	0.794	0.822	0.859	0.626	0.459
Absorbance of Transverse Axis Resonance	/	/	/	0.249	0.289	0.293	0.273	0.290

Figure 3.12 Gold nanorod growth under different pH value. (from left to right is set a to h)

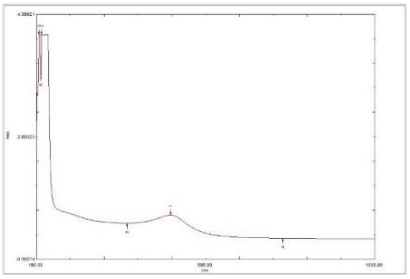

Figure 3.13a uv spectrum of rods made under 12.3 pH value

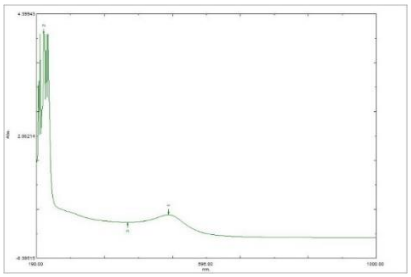

Figure 3.13b uv spectrum of rods made under 12.7 pH value

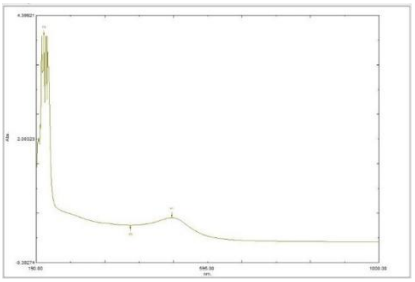

Figure 3.13c uv spectrum of rods made under 13.1 pH value

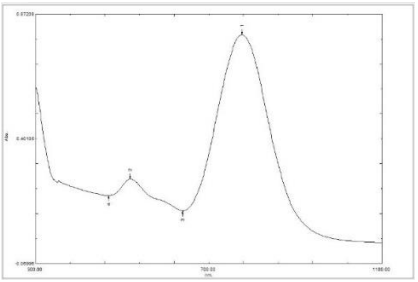

Figure 3.13d uv spectrum of rods made under 4.60 pH value (control group)

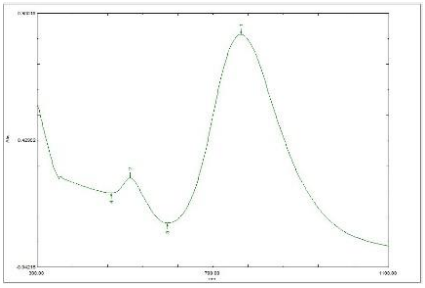

Figure 3.13e uv spectrum of rods made under 2.51pH value

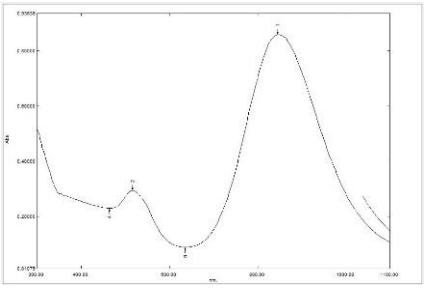

Figure 3.13f uv spectrum of rods made under 2.31pH value

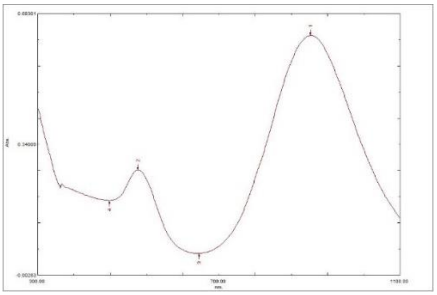

Figure 3.13g uv spectrun of rods made under 2.05 pH value

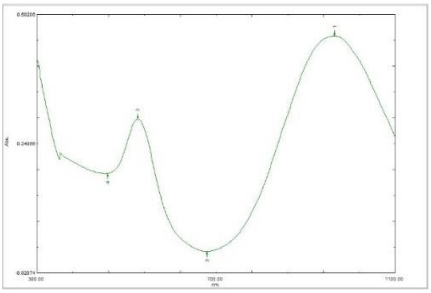

Figure 3.13h uv spectrum of rods made under 1.83 pH value

From all data, spectra and images, it is apparent that as gold seed and gold atoms growth in strong basic environment, they cannot aggregate together, forming gold nanorods. When the solution is in a more acidic

environment at first, their rods have similar length, but as more acid is added into solution the rods in this environment is much longer than the control group an obvious right shift of longitudinal axis of rods prove this. Another change is the uv-vis spectra of rods in strong acid environment are smoother. This means that a strong acid environment can successfully prevent gold solution from forming byproducts and the fusion between contact gold nanorods. Based on this result, it is possible to compare each set's absorbance of longitudinal axis. Compared control group, 0.015 and 0.025 mL HCL group, the absorbance and length of gold nanorod is keep increasing. This shows that a strong acid environment can help the rods grow more and longer. This result agree with the result I find in papers [70, 74]. For example, Qingshan Wei and his group members [70] believe that due to the pH-dependent reducing ability. The growth rate of gold nanorods is particularly slower at pH 2.5 than pH 6.7. At low pH environment (pH 2.5), Au (I) was slowly reduced to Au (0), which is helpful for the selective absorption of Au (0) to specific crystal facets of the seeds under the regulation of CTAB. Moreover, when pH is low, the inter-rod repulsion is strengthened due to the higher concentration of H^+ in solution. The fusion of two neighborhood undergrowth rods was avoided. So strong acid environment can help glod ions being reduced to gold atoms quickly and increasing the inter-rod repulsion, these two properties result in yielding better uniform, less byproducts gold nanorods.

In all, adding appropriate amount of acid is an effective way to optimize seed-mediate method of making gold nanorods and control the size of gold nanorods.

3.5.7 SEM Image of Different Gold Nanorods

This parts is designed to use SEM observing different gold nanorods. Main purpose are as followed,

1. Ensure most of particles in gold solution which are made in experiments are gold nanorods.

2. Prove the properties found in uv-vis spectra still available in SEM pictures.

3. Find the relationship between surface plasmon resonances of longitudinal axis of gold nanorods and their length that are shown in SEM images.

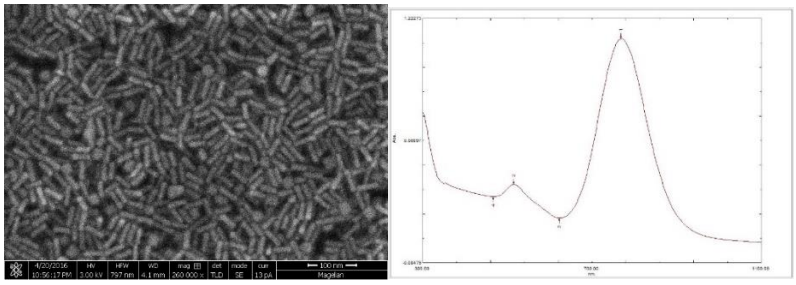

Figure 3.14a SEM image and uv-vis spectrum of standard group gold nanorod

Plasmon resonances of rod's longitudinal axis is 768nm.

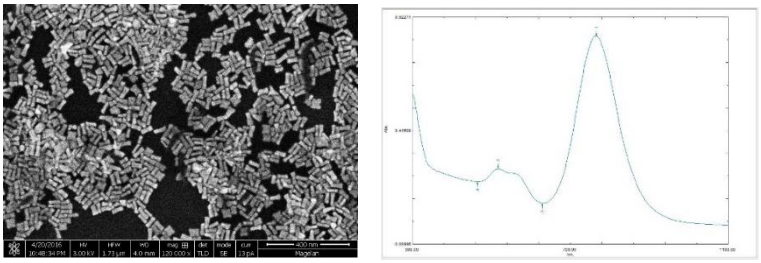

Figure 3.14b SEM image and uv-vis spectrum of gold nanorods growth with60uL AgNO3

Plasmon resonances of rod's longitudinal axis is 766nm.

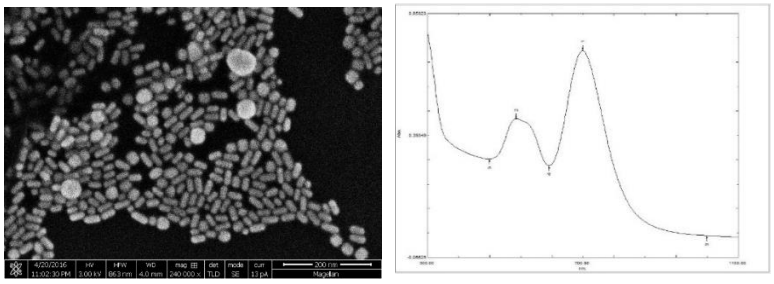

Figure 3.14c SEM image and uv-vis spectrum of gold nanorods growth with 1mL CTAB

Plasmon resonances of rod's longitudinal axis is 699nm.

Based on SEM images and uv-vis spectra, it is apparently that all three main purposes are be verified.

1. The gold naooparticles made in experiments are gold nanorods, after being observed by SEM.

2. Depending on uv-vis spectra, standard group rods and rods growth with 60uL $AgNO_3$ should have similar length and longer than the third group. This is also true in SEM images.

3. Based on uv-vis spectra, amount of byproducts should increasing as the following order, standard group, rods growth with 60uL $AgNO_3$ and rods growth with 1mL CTAB, this is also verified by SEM images.

4. Rods' length with a plasmon resonance about 770nm is 55nm, and is 43 nm with a plasmon resonance about 700nm.

3.6 Summary

Based on the experiments for CTAB and $AgNO_3$, the first mechanism is more appropriate to explain the forming process than the second mechanism. (Shown in chapter two) The first mechanism shown, briefly, CTA−Br−Ag+ capping on sides of gold nanorods, the special facets that capping agents hard to be absorbed is the longitudinal direction of rods. Second mechanism shows a UPD effect of Ag atoms and these Ag atoms can cover over gold seeds and then CTAB agents cover over Ag atoms. In my view, the difference between these two similar mechanisms is that CTAB contacts with gold seeds or Ag atoms contacts them by UPD effect.

The uv-vis spectra of different seeds' size distribution verify that if there aren't any seed in gold growth solution, it cannot form any rods or byproducts that their surface plasmon resonance peak can be detected by UV-visible spectroscopy in the range of 300nm to 1100nm. So all the byproducts be shown on the spectra is formed by irregular growth of gold nanoseeds.

Analyze the spectra of gold nanorods growth in different amount of CTAB, explaining the first mechanism, when there are insufficient amount of CTAB, this will cause lacking of CTA-Br-Ag+ capping agent in growth solution and some of seeds cannot be fully cover by agents, so they growth in random direction and size, then part of these seeds growth into byproducts with a plasmon resonance can be detected by UV-visible

spectroscopy and a large amount of byproducts are too big to be detected by uv-vis machine in range of 300 to 1100 nm. As the amount of CTAB increase the amount of byproducts decrease. So the CTAB experiment verifies the first mechanism is right. However, the second mechanism cannot be explained by this experiment. Since, first, if Ag atoms' UPD effect is the main part capping gold nanoseeds, there shouldn't so many byproducts form in the solution when CTAB is insufficient. Second, it shouldn't have an apparent positive correlation between the increasing amount of byproducts and decreasing amount of CTAB if UPD effect is primary reason for seeds' anisotropictally growth in special direction.

Analyze the spectra of gold nanorods growth in different amount of $AgNO_3$, when there isn't any silver nitrate in growth solution, a small amount of gold nanosphere have a similar size with the transverse axis of rods form in solution. Combine with the result from Kyoungweon, Wei, Edgar and Seyed-Razavi's group result [35, 36, 37, 38]. Seeds growth instropically up to 6nm size then because of capping agents, growth mostly in special facet {111}, 6nm is approximate equal to nanosphere form in no silver nitrate experimental set and transverse axis of rods. This equation proves the result [35, 36, 37, 38] is right and shows that CTAB capping agents without silver ions can cap on facets of seeds but without selectivity and efficiency compared with capping agents with Ag ions. Because spherical shape shows no selectivity and small amount shows inefficiency. This

result also be verified by this phenomenon: Using sodium citrate instead of silver nitrate need more CTAB form gold nanorods [20, 21, 22, 27]. Since this also proves that $AgNO_3$ is an effective chemical that helps CTAB capping on gold nanoseeds selectively and effectively.

When adding excess of $AgNO_3$, the first mechanism can be explained as this: extra amount of $AgNO_3$ contact with extra CTAB and these excess capping agents cover on the longitudinal axis of a small amount of seeds during their forming process causing these seeds form into byproducts. There are excess CTAB in growth solution is because 5mL is not the very exact amount of CTAB for 50uL seeds in solution, so there should have a few excess CTAB in growth solution. The second mechanism can be explained as: since the UPD effect, excess Ag atoms deposit on the longitudinal axis of a small amount of seeds during their forming process causing these seeds form into byproducts.

In short, gold nanorods growth in different amount of $AgNO_3$, this experiment cannot distinguish which mechanism is more appropriate for the forming process but it can explains the observing result [35, 36, 37, 38] is true under thesis experimental result and these two mechanism.

In all, these results and papers show the mechanism of gold nanorods' growth is this: (0−2 min): seed particles with a mixture of {100} and {111} facets isotropically grow to ~6 nm spherical nanoparticles then the CTA−Br−Ag+ face-specific capping agent acts as a face-specific capping

agents capping over most facets of gold nanoseeds and encouraging anisotropic growth in special facets {111}, and maybe there is a very small amount of seed following silver's UPD effect mechanism and this should be kept continuously research.

CHAPTER 4
ACHIEVEMENT AND FUTURE WORK

4.1 Achievements

The main achievements in this work are summarized below:

1. Gold nanorods are successfully synthesized based on the seed-mediated growth method.

2. The gold nanorod aspect ratio is tuned by varying added amounts of silver nitrate.

3. Adding appropriate amounts of acid with stirring growth solution slowly can optimize the growth of gold nanorods

4. Large size seeds form shorter gold nanorods.

5. Only adding stirring step increase amounts of byproducts.

6. CTAB can cap on facets of gold seeds but without selectivity and efficiency, Ag ions can help CTAB cap on the gold seeds selectively and effectively.

7. The mechanism of gold nanorods forming process can be described as this: first, seed particles with a mixture of {100} and {111} facets isotropically grow to ~6 nm spherical nanoparticles then the CTA−Br−Ag+ face-specific capping agent acts as a face-specific capping agent, encouraging anisotropic growth in special facets {111}.

8. Tuning aspect ratio of rods can be controlled by tuning amounts of $AgNO_3$ adding into growth solution.

9. Based on conclusions shown above, optical applications based on gold nanorods can be improved by adding appropriate amounts of acid and stirring at a low rate or using a very accurate amount of $AgNO_3$, during forming gold nanorods.

4.2 Future Work

1. Find effective way to reduce amounts of CTAB being used in seed-mediate method or replace it with other chemicals

2. Optimize other more effective way for making gold nanorods, let them replace seed-mediate method.

3. Explore more applications that using gold naorod as raw material such as etching gold naorods into small seeds and doing reductive growth to get more uniform nanoparticles with various shapes.

4. Based on conclusions shown above, future optical applications based on gold nanorods can be improved by find a more effective way to optimize seed-mediate approach based on the forming mechanism, replacing $AgNO_3$ and CTAB by other better chemicals, and trying other environments other than strong acid environment may have a breakthrough result.

Reference

1. Yevgeniy Davletshin, Modeling the optical properties of a single gold nanorod for use in biomedical applications, Ryerson University, 2010, Toronto, Ontario, Canada.
2. Maier S.A. Plasmonics: fundamentals and applications. Springer, 2007.
3. Ziyu Gu, Synthesis and Alignment of Volume and Shape Controlled Gold Nanorods, Leiden University, 2010.
4. Suryanarayana, C., The structure and properties of nanocrystalline materials: Issues and concerns. (2002), JOM Journal of the Minerals, Metals and Materials Society, 54(9): p.24-27.
5. Kuchibhatla, S.V., et al., One dimensional nanostructured materials. (2007), Progress in materials science, 52(5): p. 699-913.
6. Parkin, I.P. and R.G. Palgrave, Self-cleaning coatings. (2005), Journal of Materials Chemistry, 15(17): p. 1689-1695.
7. Becheri, A., et al., Synthesis and characterization of zinc oxide nanoparticles: application to textiles as UV-absorbers. (2008), Journal of Nanoparticle Research, 10(4): p. 679-689.
8. Fan, X., C. Xia, and R.C. Advincula, Grafting of polymers from clay nanoparticles via in situ free radical surface-initiated polymerization: Monocationic versus bicationic initiators. (2003), Langmuir, 19(10): p. 4381-4389.
9. Daniel, M.-C., D. Astruc, Gold nanoparticles: assembly, supramolecular chemistry, quantum-size-related properties, and applications toward biology, catalysis, and nanotechnology. (2004), Chemical reviews, 104(1): p. 293-346.
10. page, p.t.w.; Available from: http://periodictable.com/Elements/079/.
11. Turkevitch, J.; Stevenson, P. C.; Hillier, J., Nucleation and growth process in the synthesis of colloidal gold. (1951) Discussions of the Faraday Society, 11, 55.
12. Hu, M.; Chen, J.; Li, Z. Y.; Au, L.; Hartland, G. V.; Li, X.; Marquez, M.; Xia, Y., Gold nanostructures: engineering their plasmonic properties for biomedical applications. (2006), Chemical Society Reviews, 35, 1084-1094.
13. Olson, T. Y.; Zhang, J. Z., Structural and optical properties and emerging applications of metal nanomaterials. (2008), J Mater Sci Technol. 24 (4), 433-446.
14. Gole, A.; Murphy, C. J., Seed-mediated synthesis of gold nanorods: Role of the size and nature of the seed. (2004), Chem Mater, 16 (19), 3633-3640.
15. Ghosh, S. K.; Pal, T., Interparticle coupling effect on the surface plasmon resonance of gold nanoparticles: from theory to applications. (2007), Chem Rev, 107 (11), 4797-4862.
16. Kelly, K. L.; Coronado, E.; Zhao, L. L.; Schatz, G. C., The optical properties of metal nanoparticles: The influence of size, shape, and dielectric environment. (2003), J Phys Chem B, 107 (3), 668-677.
17. Murphy, C. J.; Gole, A. M.; Hunyadi, S. E.; Stone, J. W.; Sisco, P. N.; Alkilany, A.; Kinard, B. E.; Hankins, P., Chemical sensing and imaging with metallic nanorods. (2008), Chem Commun, (5), 544-557.
18. Murphy, C. J.; Sau, T. K.; Anand, M. G.; Orendorff, C. J.; Gao, J.; Gou, L.; Hunyadi, S. E.; Li, T., Anisotropic metal nanoparticles: synthesis, assembly, and optical applications. (2005), J Phys Chem B, 109 (29), 13857-13870.
19. Treguer-Delapierre, M.; Majimel, J.; Mornet, S.; Duguet, E.; Ravaine, S., Synthesis of non-spherical gold nanoparticles. (2008), Gold Bull, 41 (2), 195-207.

20. Perez-Juste, J.; Liz-Marzan, L. M.; Carnie, S.; Chan, D. Y. C.; Mulvaney, P. (2004) Electric-Field-Directed Growth of Gold Nanorods in Aqueous Surfactant Solutions. AdV. Funct. Mater. 14, 571-579.
21. Rodriguez-Fernandez, J.; Perez-Juste, J.; Mulvaney, P.; Liz-Marzan, L. M. J. (2005) Spatially-Directed Oxidation of Gold Nanoparticles by Au(III)−CTAB Complexes. Phys. Chem. B, 109, 14257-14261.
22. Johnson, C. J.; Dujardin, E.; Davis, S. A.; Murphy, C. J. Mann, S. J. (2002) Optical properties of composite membranes containing arrays of nanoscopic gold cylinders. Mater. Chem. 12, 1765-1770.
23. C. A. Foss, G. L. Hornyak, J. A. Stockert and C. R. Martin, J. (1992) Optical properties of composite membranes containing arrays of nanoscopic gold cylinders. Phys Chem. 96, 7497–7499.
24. C. R. Martin, (1994) Nanotubule-Based Molecular-Filtration MembranesScience. 266, 1961–1966.
25. K. B. Jirage, J. C. Hulteen and C. R. (1997) Nanotubule-Based Molecular-Filtration Membranes. Martin, Science, 278, 655–658.
26. B. M. I. van der Zande, M. R. B€ohmer, L. G. J. Fokkink and C. Sch€onenberger. (1999) Colloidal Dispersions of Gold Rods: Synthesis and Optical Properties. Langmuir, 16, 451–458.
27. Nikhil R. Jana, Latha Gearheart, and Catherine J. Murphy. (2001) J. Phys. Chem. B 105, 4065-4067
28. Tapan K. Sau and Catherine J. Murphy. (2004) Langmuir 20, 6414-6420.
29. Samuel E. Lohse and Catherine J. Murphy. (2013) The Quest for Shape Control: A History of Gold Nanorod Synthesis. Chem. Mater. 25, 1250−1261.
30. Samuel E. Lohse and Catherine J. Murphy. (2013) The Quest for Shape Control: A History of Gold Nanorod Synthesis. Chem. Mater. 25, 1250−1261.
31. Murphy, C. J.; Thompson, L. B.; Alkilany, A. M.; Sisco, P. N.; Boulos, S. P.; Sivapalan, S. T.; Yang, J. A.; Chernak, D. J.; Huang, J. J. Phys. Chem. Lett. 2010.
32. Jana, N. R. Small 2005, 1, 875−882.
33. Grzelczak, M.; Perez-Juste, J.; Mulvaney, P.; Liz-Marzan, L. M Chem. Soc. Rev. 2008, 37, 1783−1791.
34. Catherine J. Murphy, Lucas B. Thompson, Davin J. Chernak, Jie An Yang, Sean T. Sivapalan, Stefano P. Boulos, Jingyu Huang, Alaaldin M. Alkilany, Patrick N. Sisco. (2011). Gold nanorod crystal growth: From seed-mediated synthesis to nanoscale sculpting. Colloid & Interface Science 16, 128–134.
35. Seyed-Razavi, A.; Snook, I. K.; Barnard, A. S. Cryst. Growth Des. 2011, 11 (1), 158−165.
36. Wei, Z.; Qi, H.; Li, M.; Tang, B.; Zhang, Z.; Han, R.; Wang, J.; Zhao, Y. Small 2012, 8 (9), 1331−1335.
37. Edgar, J. A.; McDonagh, A. M.; Cortie, M. B. ACS Nano 2012, 6 (2), 1116−1125.
38. Kyoungweon Park, Lawrence F. Drummy, Robert C. Wadams, Hilmar Koerner, Dhriti Nepal, Laura Fabris and Richard A. Vaia, (2013), Growth Mechanism of Gold Nanorods, Chem. Mater. 25, 555−563.
39. Vivek Sharma, Kyoungweon Park, Mohan Srinivasarao, Colloidal dispersion of gold nanorods: Historical background, optical properties, seed-mediated synthesis, shape separation and self-assembly. Materials Science and Engineering R 65 (2009) 1–38.

40. E.K. Payne, K.L. Shuford, S. Park, G.C. Schatz, C.A. Mirkin, Journal of Physical Chemistry B 110 (2006) 2150–2154.
41. S.A. Maier, Plasmonics: Fundamentals and Applications, Springer, Bath, 2007.
42. G. Mie, Annalen Der Physik 25 (1908) 377–445.
43. S. Link, M.A. El-Sayed, Journal of Physical Chemistry B 103 (1999) 4212–4217.
44. Constantin Ungureanu, Raja Gopal Rayavarapu, Srirang Manohar and
Ton G. van Leeuwen. Discrete dipole approximation simulations of gold nanorod optical properties: Choice of input parameters and comparison with experiment, journal of applied physics 105, 102032 (2009).
45. M. B. Mohamed, V. Volkov, S. Link, and M. A. El-Sayed, Chem. Phys. Lett. 317, 517 2000.
46. Huang, I. H. El-Sayed, W. Qian, and M. A. El-Sayed, Nano Lett. (2007), 7, 1591.
47. S.A. Maier, H.A. Atwater, Journal of Applied Physics 98 (2005).
48. Huanjun Chen, Lei Shao, Qian Lia and Jianfang Wang, Gold nanorods and their plasmonic properties, Chem. Soc. Rev., 2013, 42, 2679—2724.
49. P. K. Jain, K. S. Lee, I. H. El-Sayed and M. A. El-Sayed, J. Phys. Chem. B, 2006, 110, 7238.
50. T. Ming, H. J. Chen, R. B. Jiang, Q. Li and J. F. Wang, J. Phys. Chem. Lett., 2012, 3, 191.
51. C. X. Yu and J. Irudayaraj, Biophys. J., 2007, 93, 3684.
52. M. P. Kreuzer, R. Quidant, G. Badenes and M.-P. Marco, Biosens. Bioelectron., 2006, 21, 1345.
53. P. Pramod, S. T. S. Joseph and K. G. Thomas, J. Am. Chem. Soc., 2007, 129, 6712.
54. J. Kumar and K. G. Thomas, J. Phys. Chem. Lett., 2011, 2, 610.
55. J. Jiang, K. Bosnick, M. Maillard and L. Brus, J. Phys. Chem. B, 2003, 107, 9964.
56. N. R. Jana and T. Pal, Adv. Mater., 2007, 19, 1761.
57. A. Lee, G. F. S. Andrade, A. Ahmed, M. L. Souza, N. Coombs, E. Tumarkin, K. Liu, R. Gordon, A. G. Brolo and E. Kumacheva, J. Am. Chem. Soc., 2011, 133, 7563.
58. G. von Maltzahn, A. Centrone, J.-H. Park, R. Ramanathan, M. J. Sailor, T. A. Hatton and S. N. Bhatia, Adv. Mater., 2009, 21, 3175.
59. N. Engheta and R. W. Ziolkowski, Metamaterials: Physics and Engineering Explorations, Wiley-IEEE Press, 2006.
60. J. Valentine, S. Zhang, T. Zentgraf, E. Ulin-Avila, D. A. Genov, G. Bartal and X. Zhang, Nature, 2008, 455, 376.
61. N. Liu, L. Langguth, T. Weiss, J. Ka ̈stel, M. Fleischhauer, T. Pfau and H. Giessen, Nat. Mater., 2009, 8, 758.
62. S. Zhang, D. A. Genov, Y. Wang, M. Liu and X. Zhang, Phys. Rev. Lett., 2008, 101, 047401.
63. Y. Nishijima, K. Ueno, Y. Yokota, K. Murakoshi and H. Misawa, J. Phys. Chem. Lett., 2010, 1, 2031.
64. Y. Nishijima, K. Ueno, Y. Kotake, K. Murakoshi, H. Inoue and H. Misawa, J. Phys. Chem. Lett., 2012, 3, 1248.
65. Tapan K. Sau and Catherine J. Murphy. (2004). Seeded High Yield Synthesis of Short Au Nanorods in Aqueous Solution. Langmuir, 20, 6414-6420.
66. Mingzhao Liu and Philippe Guyot-Sionnest. (2005). Mechanism of Silver(I)-Assisted Growth of Gold Nanorods and Bipyramids. J. Phys. Chem. B, 109, 22192-22200.
67. Carlo Morasso , Silvia Picciolini , Domitilla Schiumarini, Dora Mehn , Isaac Ojea-Jime ́nez , Giuliano Zanchetta , Renzo Vanna , Marzia Bedoni , Davide Prosperi, Furio Gramatica. (2015).

Control of size and aspect ratio in hydroquinone-based synthesis of gold nanorods. Springer Science. DOI 10.1007/s11051-015-3136-9.
68. Qiaoling Li and Yahong Cao (2012). Preparation and Characterization of Gold Nanorods, Nanorods, Dr. Orhan Yalçın (Ed.), ISBN: 978-953-51-0209-0, InTech, DOI: 10.5772/35880.
69. Seyyed Mohammad Hossein Abtahi. (2013). Synthesis and Characterization of Metallic Nanoparticles with Photoactivated Surface Chemistries.
70. Qingshan Wei, Jian Ji, and Jiacong Shen. (2008). pH Controlled Synthesis of High Aspect-Ratio Gold Nanorods. Nanoscience and Nanotechnology. Vol.8, 5708–5714.
71. Zhenhua Sun, Weihai Ni, Zhi Yang, Xiaoshan Kou, Li Li, and Jianfang Wang. (2008). pH-Controlled Reversible Assembly and Disassembly of Gold Nanorods. Small. DOI: 10.1002/smll.200800099
72. Marek Grzelczak,a Jorge Pe ŕez-Juste, Paul Mulvaney and Luis M. Liz-Marzan. (2008 July 7). Shape control in gold nanoparticle synthesis. Chem. Soc. Rev. 37, 1783–1791.
73. Kenji Okitsu, Kohei Sharyo and Rokuro Nishimura. (2009). One-Pot Synthesis of Gold Nanorods by Ultrasonic Irradiation: The Effect of pH on the Shape of the Gold Nanorods and Nanoparticles. Langmuir. 25 (14), pp 7786–7790.
74. Yang Qiu, Ying Liu, Liming Wang, Ligeng Xu, Ru Bai a, Yinglu Ji, Xiaochun Wu, Yuliang Zhao, Yufeng Li, Chunying Chen. (2010). Surface chemistry and aspect ratio mediated cellular uptake of Au nanorods. Biomaterials 31, 7606-7619.